ORIGINAL ARTICLE

Suitability assessment of non-destructive testing for mechanical property estimation of concrete with wind turbine wastes

Víctor Revilla-Cuesta · Manuel Hernando-Revenga · Marta Skaf · Ana B. Espinosa

Received: 30 October 2025 / Revised: 30 October 2025 / Accepted: 17 January 2026

Abstract
The simultaneous use of Coarse Recycled Aggregate (CRA) and Raw-Crushed Wind-Turbine Blade (RCWTB) in concrete enables the recycling and revaluation of two wastes from wind-farm decommissioning. Verification of the validity of Non-Destructive Testing (NDT) for field control of the concrete mixes produced with these wastes is key to extending its possibilities of use, as is the application of NDT in concrete monitoring. This research evaluates the suitability of Ultrasonic Pulse Velocity (UPV) and rebound index to estimate the mechanical properties of concrete made with up to 100% CRA and 10% RCWTB. From an experimental approach, both NDT properties decreased when adding both wastes, although rebound index exhibited a higher experimental variability. These experimental results were subsequently analyzed through two statistical procedures. First, an analysis through response surface methodology was conducted, whose models revealed that the directions of maximum variation (gradients) for UPV, modulus of elasticity, compressive strength and tensile splitting strength were aligned, especially for high waste contents. Second, a regression analysis determined that only these three mechanical properties could be properly estimated using these NDT properties, since Poisson's coefficient and flexural strength largely depended on the stitching of the cementitious matrix, influenced by the fibers from glass fiber-reinforced polymer contained in RCWTB. UPV was always the NDT property that yielded more accurate estimations, while rebound index only improved the estimation quality of compressive strength, although a reduction of its measured value is recommended to avoid strength overestimations. In general, non-linear multiple regression models provided accurate and reliable predictions.

Keywords Concrete · Wind-turbine blade waste · Coarse recycled aggregate · Non-destructive testing · Mechanical properties

Abbreviations

CCD	Central composite design
CNA	Coarse natural aggregate
CRA	Coarse recycled aggregate
GFRP	Glass fiber-reinforced polymer
ITZ	Interfacial transition zones

Published online: 11 February 2026

NDT	Non-destructive testing
RCWTB	Raw-crushed wind-turbine blade
RSM	Response surface methodology
UPV	Ultrasonic pulse velocity

1 Introduction

Coarse Recycled Aggregate (CRA) is one of the main alternatives to reduce the large consumption of Coarse Natural Aggregate (CNA) in concrete production, which reaches 50 billion tons per year worldwide [1]. This type of aggregate comes from the crushing of out-of-use concrete elements and consists of CNA with bonded mortar. This adhered mortar causes CRA to have less density than CNA, which leads to a less dense concrete [2], and a higher water absorption capacity, which results in reduced workability of concrete [3]. In addition, CRA also creates double interfacial transition zones (ITZ) in hardened concrete: first between the CNA and the bonded mortar, and second between the bonded mortar and the new cementitious matrix [4]. This usually results in a worsening of concrete strength, as CRA favors aggregate debonding from the matrix when loading occurs [5], and durability resistance, as CRA creates more porous and crack-prone ITZ that facilitate the entry of damaging external agents [6]. Finally, CRA is also more flexible than CNA, which increases the deformability and shrinkage of concrete [7].

The negative impacts of CRA can be partially offset with appropriate CRA production procedures [8], and adjusting the concrete composition by increasing the contents of water, and plasticizing and water-reducing admixtures [9]. Another possibility investigated to minimize the impact of CRA on the hardened behavior of concrete is its joint use with fibers, since they have opposite effects to CRA in several regards [10]. On the one hand, fibers reduce concrete shrinkage acting as rigid elements that oppose the contraction of the cementitious matrix [11]. On the other hand, fibers' stitching reduces cracking, thus improving durability and load-bearing capacity after failure [12]. Finally, they exert a confining effect that can increase the stiffness and strength of concrete under compressive loads [13]. Traditionally, steel fibers have been mostly used due to their high elastic stiffness [14]. However, their manufacturing process generates large sustainability impacts, their use in concrete counterbalancing the environmental benefits of CRA addition [14]. Therefore, feasibility of sustainable fiber usage, both recycled and natural, in concrete is being researched [12].

One widely used material in several fields is Glass Fiber-Reinforced Polymer (GFRP), which is composed of glass fibers parallelly embedded in an epoxy matrix [15]. GFRP has many engineering applications due to its high tensile strength and low weight, being widely used in automotive and aeronautic industries, among others [16]. In fact, GFRP is a fundamental component of wind-turbine blades [17]. However, GFRP also has drawbacks, mainly related to its recycling, for which there is no widely accepted solution [16]. One possibility is the separation of the fiberglass and the epoxy matrix by pyrolysis (application of heat to burn the matrix) or solvolysis (use of solvents to dissolve the epoxy matrix) [15]. However, these processes are environmentally damaging, costly and often lead to a significant deterioration of the mechanical characteristics of the fiberglass [18]. Currently, efforts are being conducted to fine-tune such treatments [19]. Another possibility, addressed in this paper, is the crushing of end-of-life GFRP to obtain recycled fibers that can be added to concrete [20]. GFRP fibers provide concrete with the advantages described above [21], being also effective in concrete containing CRA [22].

Focusing on the wind-energy sector, a major source of GFRP needing to be recycled [23], two aspects are noteworthy. First, the dismantling of wind farms not only generates significant amounts of GFRP from wind-turbine blades that required recycling, but also produces CRA from the demolition of the surface layer of wind-turbine footings [24]. Thus, the successful joint use of CRA and recycled GFRP fibers in concrete allows the simultaneous management of these two wastes and is therefore a possible course of action that merits detailed investigation. Second, wind-turbine blades to be recycled are not only composed of GFRP, but also contain other components

such as balsa wood, which lightens the structure while providing the necessary strength [25], and polymers that coat the outside of the blade, glue elements together, and even act as stiffeners [17]. The exclusive recycling of GFRP poses the problem of looking for environmentally friendly ways to treat these other components [26]. Faced with this situation, a line of research has arisen to recycle all the elements of wind-turbine blades simultaneously through their non-selective crushing [27], yielding Raw-Crushed Wind-Turbine Blade (RCWTB), and adding it to concrete [28]. It is demonstrated that structural concrete can be successfully developed when adding this residue [29], which is composed of GFRP fibers and particles of polymers and balsa wood [28]. Moreover, the effect of the GFRP fibers it contains remains effective in counteracting the disadvantages in terms of shrinkage and cracking that the use of CRA entails [24, 30].

Non-Destructive Testing (NDT) of concrete has traditionally been conducted by evaluating the propagation velocity of ultrasonic waves within it, yielding an NDT measurement known as Ultrasonic Pulse Velocity (UPV) [31], or its surface hardness using the Schmidt hammer, value referred to as rebound index [32]. These NDT measurements enable quality assessment [33] and estimation of the mechanical behavior of concrete already in place for quality controls or rehabilitation works [34], without the need for destructive testing [35]. The usefulness and relevance of NDT has led its validity in concrete made with alternative raw materials to be detailly investigated [36]. If traditional NDT procedures prove valid, the use of non-conventional concrete can be more easily promoted. Thus, on the one hand, research on concrete with CRA has shown that this aggregate decreases UPV and rebound index due to its lower density and hardness [37], greater flexibility [38] and the weaker ITZ it generates compared to CNA [39]. Since CRA typically causes a worsening of the mechanical properties of concrete, they can be accurately estimated through NDT [40]. On the other hand, the stitching of the cementitious matrix by the fibers is hard to be evaluated by UPV and rebound index [41]. These NDT measures are mainly suitable for estimating compression-related properties when fiber addition involves other modifications in concrete composition, such as an increase in water amount [42].

From the above, the observed trends in NDT of concrete containing CRA may be altered by the simultaneous addition of RCWTB. This waste not only contains GFRP fibers, but also particles of reduced density and hardness that cause the effect of RCWTB on UPV and rebound index of concrete with CRA to be even more unclear. Faced with this situation, this research delves into the NDT evaluation of concrete made with up to 100% CRA and 10% RCWTB, an aspect that has not been covered in the scientific literature to date. Starting from experimental results of all the mechanical properties of such concrete mixes, as well as UPV and rebound index, two powerful statistical procedures such as Response Surface Methodology (RSM) and non-linear multiple regression are applied in this research to determine which mechanical properties can be estimated through these two NDT measurements. In this way, the feasibility of using NDT to analyze concrete made simultaneously with two different wastes from wind-farm decommissioning is addressed, which in turn promotes their simultaneous management through concrete production.

2 Materials and methods

2.1 Concrete components

Non-waste concrete components were CEM II/A-L 42.5 R cement (limestone content between 6 and 20% by weight) as per EN 197–1 [43], potable water, superplasticizers, siliceous aggregate divided into fractions 0–4 mm, 4–12 mm and 12–22 mm, and limestone aggregate 0–2 mm. The aggregates had a density of around 2.60 kg/dm^3 and a water absorption in the order of 0.10–0.60% by weight as per EN 1097–6 [43]. All these raw materials met the requirements of European regulations, Eurocode 2 [44], for concrete manufacture.

The first waste incorporated in the concrete mixes of this research was CRA 4–22 mm. Concrete pieces with a minimum compressive strength of 45 MPa were crushed and screened to manufacture such aggregate. Laboratory tests following EN 1097–6 [43] revealed that density and water absorption values were 2.44 kg/m^3 and 6.12%

by weight, respectively. According to the scientific literature [2, 8], the strength of the parent concrete as well as the density and water absorption values were adequate for the development of structural concrete through the addition of this CRA.

The second waste considered in this research was RCWTB, for which a detailed characterization can be found in a previous publication [28]. This waste came from the non-selective crushing of panels of wind-turbine blades, resulting in a mixed composition consisting of five constituents: GFRP fibers, GFRP micro-fibers, polymeric particles, balsa-wood particles, and a mixture of non-mechanically separable particles of all these constituents. Their proportions by weight were 66.8%, 13.0%, 8.3%, 6.3%, and 5.6%, respectively. The variability of the characteristics of the RCWTB constituents can be perceived in their differences in size and density. Thus, the GFRP fibers had an average length of 13.1 mm, an aspect ratio of 18 units and a density of 2.04 kg/dm^3, while the balsa-wood particles had a semi-spherical shape with an average size of 5 mm and a density of 0.33 kg/dm^3. RCWTB as a whole had a density of 1.63 kg/dm^3 according to EN 1097–6 [43].

2.2 Mix design

2.2.1 Central composite design (CCD)

The waste contents to be added to concrete in this research were set between 0 and 100% for CRA and between 0 and 10% for RCWTB. These amounts were established in accordance with previous research in which proper concrete performance was achieved with such residues [9, 28]. To comprehensively assess all possible combinations of CRA and RCWTB contents in concrete, a CCD with two independent variables (CRA content and RCWTB amount) was conducted to provide a solid basis for the statistical methods applied in the analysis. The usefulness of this design procedure was supported by its widespread and successful use in the assessment of concrete performance through statistical approaches [45]. To provide the statistical analyses with an even broader basis, two α values, ± 0.5 and ± 1, were considered in the CCD, the resulting waste combinations being shown in Table 1. Finally, four replicates (four concrete mixes with exactly the same composition) for the central combination of wastes (50% CRA and 5% RCWTB) were conducted to evaluate the variability of concrete behavior. Sixteen concrete mixes were produced in total, including the four replicates with the central combination of wastes.

2.2.2 Concrete composition

First, the reference concrete mix was prepared, which did not contain any waste (0% CRA and 0% RCWTB). This mix was initially designed following the indications of Eurocode 2 [44] and a granulometric adjustment to the Fuller's curve. Thus, the contents of the raw materials per cubic meter of concrete were the following: 320 kg of cement, 128 kg of water (water-to-cement ratio of 0.40), 3.20 kg of superplasticizers (1% of the cement mass), 780 kg of siliceous aggregate 12–22 mm, 555 kg of siliceous aggregate 4–12 mm, 385 kg of siliceous aggregate 0–4 mm, and 280 kg of siliceous aggregate 0–2 mm. This mix design resulted in concrete with a slump class S3 (slump of 12.5 ± 2.5 cm) as per EN 206 [43] and a compressive strength of around 45 MPa.

The addition of both wastes into concrete, CRA and RCWTB, was performed by applying volume corrections and modifying the water-to-cement ratio and the proportion of superplasticizers so that all mixes reached an S3

Table 1 CCD combinations (combinations of wastes for an α value of ± 0.5 identified with *0.5* and for an α value of ± 1 with 1)

	0% RCWTB	2.5% RCWTB	5% RCWTB	7.5% RCWTB	10% RCWTB
0% CRA	0.5, 1		1		0.5, 1
25% CRA			0.5		
50% CRA	1	0.5	0.5, 1 *	0.5	1
75% CRA			0.5		
100% CRA	0.5, 1		1		0.5, 1

*Four replicates with the central combination of wastes (50% CRA and 5% RCWTB) were performed

slump class according to EN 206 [43]. Thus, all the mixes showed the same compactability when the specimens for the hardened tests were cast, the results between mixes being therefore fully comparable. The guidelines followed for the addition of the wastes to concrete were as follows:

- CRA 4–22 mm was added by replacing CNA 4–22 mm by volume. The incorporation of CRA to concrete was combined with an increase in the water content of 7 l/m^3 for every 25%-CRA step, thus compensating for the high water-absorption levels of this non-conventional aggregate [3].
- RCWTB was added to concrete as a simultaneous replacement of all the aggregate fractions by volume, without altering the proportions between them. The presence of GFRP fibers in this waste hindered the dragging of the larger aggregate particles, which in turn reduced concrete slump [46]. Thus, the content of superplasticizers was adjusted in the concrete mixes with 10% RCWTB, so that 4.02 kg/m^3 of superplasticizers were added when such RCWTB content was not combined with CRA, and 4.26 kg/m^3 when combined with 50% and 100% CRA.

2.3 Research methodology

Based on the established mix design, nine 10 × 20-cm cylindrical, three 10 × 10x10-cm cubic and three 7.5 × 7.5x27.5-cm prismatic specimens were prepared per concrete mix. Each test result for every mix was defined as the arithmetic mean of the results of three specimens. These specimens were cured in a humid chamber at a temperature of 20 ± 2 °C and a relative humidity of 90 ± 5% until 28 days, age at which the hardened tests were performed. These tests covered both mechanical (compressive strength, modulus of elasticity, Poisson's coefficient, tensile splitting strength and flexural strength) and NDT (UPV and rebound index) properties of the mixtures. All mechanical properties were measured according to EN 12390 standards on the mechanical properties of concrete [43], while EN 12504 standards on NDT of concrete [43] were applied for UPV and rebound index. The UPV was determined by the direct method, placing the ultrasonic emitter and receiver on opposite faces of cubic specimens [42], while the rebound index was measured on the cylindrical specimens subsequently tested to compressive strength.

From all experimental results, the validity of UPV and rebound index to evaluate the mechanical behavior of concrete made simultaneously with CRA and RCWTB was analyzed using two statistical procedures:

- First, RSM was applied, developing models for the evolution of both mechanical and NDT properties as a function of the content of both wastes in concrete. Directions of maximum variation and maximum/minimum points could then be compared [45].
- Second, a regression analysis was conducted in which the mechanical properties were expressed as a function of the NDT measurements. Correlations, simple regression, linear multiple regression and finally non-linear multiple regression were considered. This enabled to verify the suitability of the NDT properties for estimating each mechanical property when used both individually and jointly [40].

Figure 1 provides an overview of the research methodology followed. Further details on the statistical analyses conducted are shown in the sections specifically dealing with each of them.

3 Results and discussion: experimental results

3.1 Mechanical properties

The average values and the standard deviations of the mechanical properties are listed in Table 2. From an overall approach, all the mixes widely fulfilled the requirements of structural concrete [44], except when jointly adding 100% CRA and 10% RCWTB. The simultaneous use of high amounts of both wastes did cause a noticeable

 https://doi.org/10.1007/s43452-026-01442-4

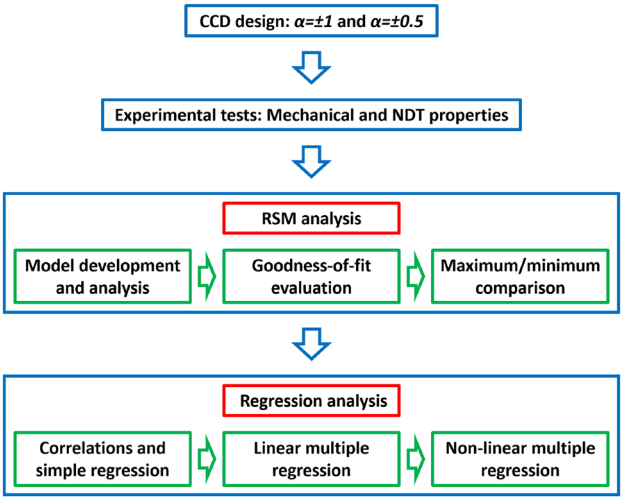

Fig. 1 Research methodology

Table 2 Average values and standard deviations of the mechanical properties of the concrete mixes

RCWTB content (%)	CRA content (%)	Compressive strength (MPa)	Modulus of elasticity (GPa)	Poisson's coefficient	Tensile splitting strength (MPa)	Flexural strength (MPa)
0	0	47.2±3.4	45.3±0.9	0.167±0.015	3.77±0.22	5.59±0.52
0	50	48.2±1.6	40.0±1.8	0.164±0.013	3.50±0.25	5.64±0.56
0	100	43.7±1.3	32.8±0.6	0.184±0.028	3.37±0.50	4.46±0.58
2.5	50	39.5±1.0	35.7±1.4	0.151±0.005	3.29±0.09	5.42±0.50
5	0	40.9±4.0	37.9±1.8	0.161±0.008	3.68±0.36	5.91±0.56
5	25	45.0±1.8	38.3±1.7	0.188±0.043	3.59±0.36	5.44±0.45
5 *	50 *	41.9±1.7	34.1±1.6	0.157±0.011	3.53±0.31	5.28±0.28
5	75	36.7±1.8	32.6±1.0	0.165±0.010	3.45±0.08	5.51±0.21
5	100	36.7±3.6	27.9±0.4	0.164±0.015	2.88±0.37	4.76±0.13
7.5	50	38.9±1.9	32.1±1.2	0.183±0.022	3.05±0.29	5.26±0.07
10	0	39.3±2.8	33.8±0.7	0.183±0.011	3.64±0.25	5.44±0.35
10	50	42.5±0.8	28.6±0.4	0.192±0.030	3.79±0.24	6.41±0.34
10	100	26.8±2.1	23.7±0.7	0.182±0.016	2.60±0.08	4.88±0.28

*The values for the concrete with 5% RCWTB and 50% CRA were obtained through the average of the results of four different mixes with exactly the same composition and those waste contents

deterioration of the mechanical behavior of concrete. In fact, the value of 25 MPa, which is the minimum compressive strength accepted to consider a concrete for structural use [44], was reached by a narrow margin with these specific waste amounts. Finally, it should be noted that the standard deviations were adequate for statistical modeling based on the results obtained [29, 38].

The addition of CRA led to a general decreasing trend of all the mechanical properties. Thus, the addition of 100% CRA led to reductions in compressive strength, modulus of elasticity, tensile splitting strength and flexural strength of 7.4%, 27.6%, 10.6% and 20.2%, respectively, in concrete that did not incorporate RCWTB. These decreases were 31.8%, 29.9%, 28.6% and 10.3%, respectively, when 100% CRA was added to concrete made with 10% RCWTB. The reductions caused by CRA were due to its higher flexibility and worse adhesion to the cementitious matrix than CNA [5, 7], both phenomena caused by the presence of adhered mortar [4]. Furthermore, these phenomena were amplified when their effect was joined with those derived from the weak and deformable particles present in the RCWTB [47, 48], since compressive strength, modulus of elasticity and tensile splitting strength experienced greater decreases when combining both residues. However, as reported in other research [22], it should be noted that the stitching of the cementitious matrix by the GFRP fibers was effective in limiting

Table 3 Average values and standard deviations of the NDT properties of the concrete mixes

RCWTB content (%)	CRA content (%)	UPV (km/s)	Rebound index
0	0	4.88±0.09	37.3±1.2
0	50	4.73±0.03	36.7±0.6
0	100	4.48±0.06	37.0±1.0
2.5	50	4.52±0.01	33.7±0.6
5	0	4.65±0.08	36.3±0.6
5	25	4.55±0.06	35.0±0.0
5*	50*	4.55±0.07	35.5±0.8
5	75	4.46±0.03	35.3±2.3
5	100	4.37±0.02	36.0±0.0
7.5	50	4.50±0.01	36.3±0.6
10	0	4.63±0.08	33.7±2.3
10	50	4.43±0.05	37.0±1.0
10	100	4.19±0.11	32.0±2.0

*The values for the concrete with 5% RCWTB and 50% CRA were obtained through the average of the results of four different mixes with exactly the same composition and those waste contents

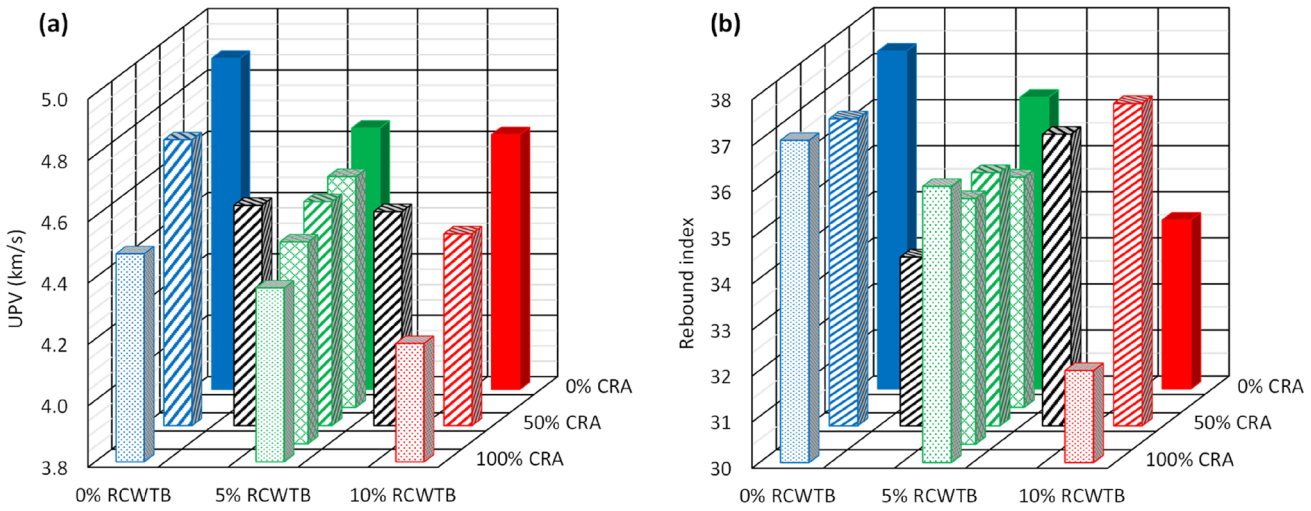

Fig. 2 Values of NDT properties: (a) UPV; (b) rebound index

the loss of flexural strength when CRA was added. This effect was especially pronounced when combined with 50% CRA, likely due to the friction of some of these fibers with rough CRA particles [24].

The use of RCWTB also affected the mechanical behavior of concrete. Thus, the addition of 10% RCWTB to concrete without any CRA caused losses in compressive strength and modulus of elasticity of 16.7% and 25.4%, respectively, due to the high deformability and poor adhesion of the polymeric and balsa-wood particles present in this waste to the cementitious matrix [47, 48]. However, tensile splitting strength and flexural strength only diminished by 3.4% and 2.7%, respectively, the negative effect of these particles being effectively compensated by the GFRP fibers' stitching [26]. When combined with CRA, the RCWTB effect was maintained, and even the flexural strength was improved, for instance, by 8.6% in a concrete mix with 100% CRA when 10% RCWTB was added. Finally, it should be noted that none of the two wastes significantly modified Poisson's coefficient, no clear trend being found.

3.2 NDT properties

The values of the NDT properties, UPV and rebound index, are detailed in Table 3, while Fig. 2 shows their evolution with the variation of the content of both wastes. Both NDT properties had values within the expected

ranges for their compressive strengths [32], as well as standard deviations suitable for statistical modeling [38]. However, the trends shown by each NDT property were different:

- UPV (Fig. 2a) was clearly reduced when increasing the content of any waste. For example, the addition of 100% CRA reduced UPV in the range of 6–10% regardless of the RCWTB content. Similarly, the incorporation of RCWTB to concrete with any CRA amount decreased UPV around 5–6%. Both the CRA and the particles of polymers and balsa wood within RCWTB have a lower density and stiffness than natural aggregate [39, 47]. Dense and stiff raw materials usually lead to a high UPV in concrete [35], so the addition of both wastes clearly contributed to the decrease of this NDT property. The increase in porosity caused by these wastes could also partially contribute to such UPV reduction [6, 28]. Finally, it should be noted that the decrease due to RCWTB was lower, as the GFRP fibers acted as ultrasound conductors, with an UPV in the fiber direction of 2–3 km/s [49].
- Rebound index (Fig. 2b) tends to exhibit an appreciable variability [32], as also demonstrated the absence of a clear trend of variation of this NDT property when incorporating both wastes. On the one hand, the addition of RCWTB reduced the rebound index, especially in concrete with only one type of coarse aggregate (0% CRA, *i.e.*, 100% CNA, and 100% CRA), because of the deformable and weak particles that it contained [47, 48]. On the other hand, CRA addition did not reveal a marked trend, the rebound index therefore remaining approximately constant. It seems that CRA only noticeably affected the rebound index when a significant proportion of bonded mortar was close to the specimen surface, thus affecting the surface hardness [37, 39], which endowed this NDT property with a high degree of randomness.

4 Results and discussion: RSM analysis

4.1 Overview

The validity of UPV and rebound index to approach the mechanical properties of concrete produced simultaneously with CRA and RCWTB was first evaluated through an RSM analysis. For this purpose, a quadratic model was developed for each mechanical and NDT property and each α value, ± 0.5 and ± 1, using the software Design Expert [50]. These models depended on the first and second powers of the contents of both wastes, as well as the interaction between them. The developed models were fitted according to Eq. (1), in which P was the property considered (in MPa for compressive strength, tensile splitting strength and flexural strength; in GPa for modulus of elasticity; in km/s for UPV; and dimensionless for Poisson's coefficient and rebound index); C_{RCWTB} was the RCWTB content added to the concrete mix in percentage; C_{CRA} was the CRA content added to the concrete mix in percentage; and β were least-square adjustment coefficients.

$$\begin{aligned} P = & \beta_0 + \beta_{RCWTB} \cdot C_{RCWTB} + \beta_{CRA} \cdot C_{CRA} \\ & + \beta_{RCWTB \cdot CRA} \cdot C_{RCWTB} \cdot C_{CRA} \\ & + \beta_{RCWTB^2} \cdot C_{RCWTB}^2 + \beta_{CRA^2} \cdot C_{CRA}^2 \end{aligned} \tag{1}$$

Then, the goodness-of-fit of the two models developed for each property (one model for each α value) was compared. It was analyzed the significance of the model, a p-value greater than 0.05 indicating that the model was significant at a 95% confidence level [5]; the percentage of variance described through the R^2 coefficient; and the lack of fit based on the variability of the concrete mix with the central combination of wastes (50% CRA and 5% RCWTB), a p-value greater than 0.05 revealing absence of lack of fit at a 95% confidence level [51]. From this evaluation, the optimum α value for the RSM analysis was established, the random distribution of the residuals for the optimum models being subsequently verified.

Once the models were defined, the directions of maximum variation (gradients) and the maximum and minimum points of the models for the NDT properties were compared with those of the models for the mechanical

Table 4 Goodness-of-fit analysis of RSM models

Property	$\alpha = \pm 1$			$\alpha = \pm 0.5$		
	Model *p*-value	R^2 (%)	Lack-of fit *p*-value	Model *p*-value	R^2 (%)	Lack-of fit *p*-value
Compressive strength	0.0299	82.18	0.6358	0.0436	79.58	0.6119
Modulus of elasticity	0.0000	98.23	0.8469	0.0001	97.41	0.7777
Poisson's coefficient	0.1433	67.96	0.8417	0.5961	39.53	0.3452
Tensile splitting strength	0.0703	75.62	0.5214	0.0521	78.20	0.7718
Flexural strength	0.0953	67.78	0.1334	0.1288	69.27	0.5143
UPV	0.0017	93.48	0.7463	0.0075	89.08	0.5552
Rebound index	0.3322	54.53	0.0628	0.3172	55.45	0.0731

Table 5 Adjustment coefficients (β) for optimum RSM models ($\alpha = \pm 1$) according to Eq. (1)

Property	β_0	β_{RCWTB}	β_{CRA}	$\beta_{RCWTB \cdot CRA}$	β_{RCWTB^2}	β_{CRA^2}
Compressive strength	45.95000	-1.34667	0.16167	-0.00900	0.07800	-0.00184
Modulus of elasticity	45.13750	-1.43167	-0.08917	0.00240	0.02450	-0.00032
Poisson's coefficient	0.16508	-0.00520	0.00002	-0.00002	0.00075	0.00000
Tensile splitting strength	3.66833	-0.02433	0.00673	-0.00064	0.00360	-0.00011
Flexural strength	5.70042	-0.09533	0.00513	0.00057	0.01015	-0.00017
UPV	4.86417	-0.04300	-0.00243	-0.00004	0.00170	-0.00001
Rebound index	36.83333	-0.24667	0.02333	-0.00140	0.00400	-0.00024

properties. A coincidence in these aspects between the model for an NDT property and the model for a mechanical property was indicative that both properties followed the same trends when wastes were incorporated into concrete, so they might be closely related [45].

4.2 Model definition

Table 4 lists the goodness-of-fit parameters of the RSM quadratic models developed for each α value, which showed no lack of fit in any case. The performance detected for each property was the following:

- Compressive strength, modulus of elasticity and UPV were the properties that were best fit by RSM. Their models were significant for both α values and exhibited the highest R^2 coefficients, with minimum values of around 80%.
- Tensile splitting strength and flexural strength were less accurately fitted, with RSM models generally not significant at a 95% confidence level, but with R^2 coefficients of intermediate value, between 65 and 80%. It is thought that the stitching effect of GFRP fibers could not be fully adequately simulated through RSM due to its different effect for each CRA amount [24]. In fact, their best interaction was found with 50% CRA. However, the models developed for an α value of ± 1 were significant at a 90% confidence level (model *p*-value lower tan 0.10), which for an α value of ± 0.5 were not.
- Finally, the large experimental dispersion of the Poisson's coefficient and the rebound index meant that the RSM models for these properties were not significant in any case [51]. Furthermore, they exhibited very low R^2 values, on average around 55%.

Based on all the above aspects, an α value of ± 1 was considered the most appropriate for the RSM analysis. This value allowed the development of significant quadratic models for compressive strength, modulus of elasticity and UPV, with R^2 coefficients of 82% for compressive strength and over 90% for modulus of elasticity and UPV. In addition, it allowed the development of significant models for tensile splitting strength and flexural strength at a 90% confidence level with intermediate R^2 coefficients. The values of the β adjustment coefficients of these models are detailed in Table 5, which reveal that the models mainly depended on the first-power and interaction terms, the second-power terms providing the models with descriptive curvatures [45]. Finally, it should be noted

 https://doi.org/10.1007/s43452-026-01442-4

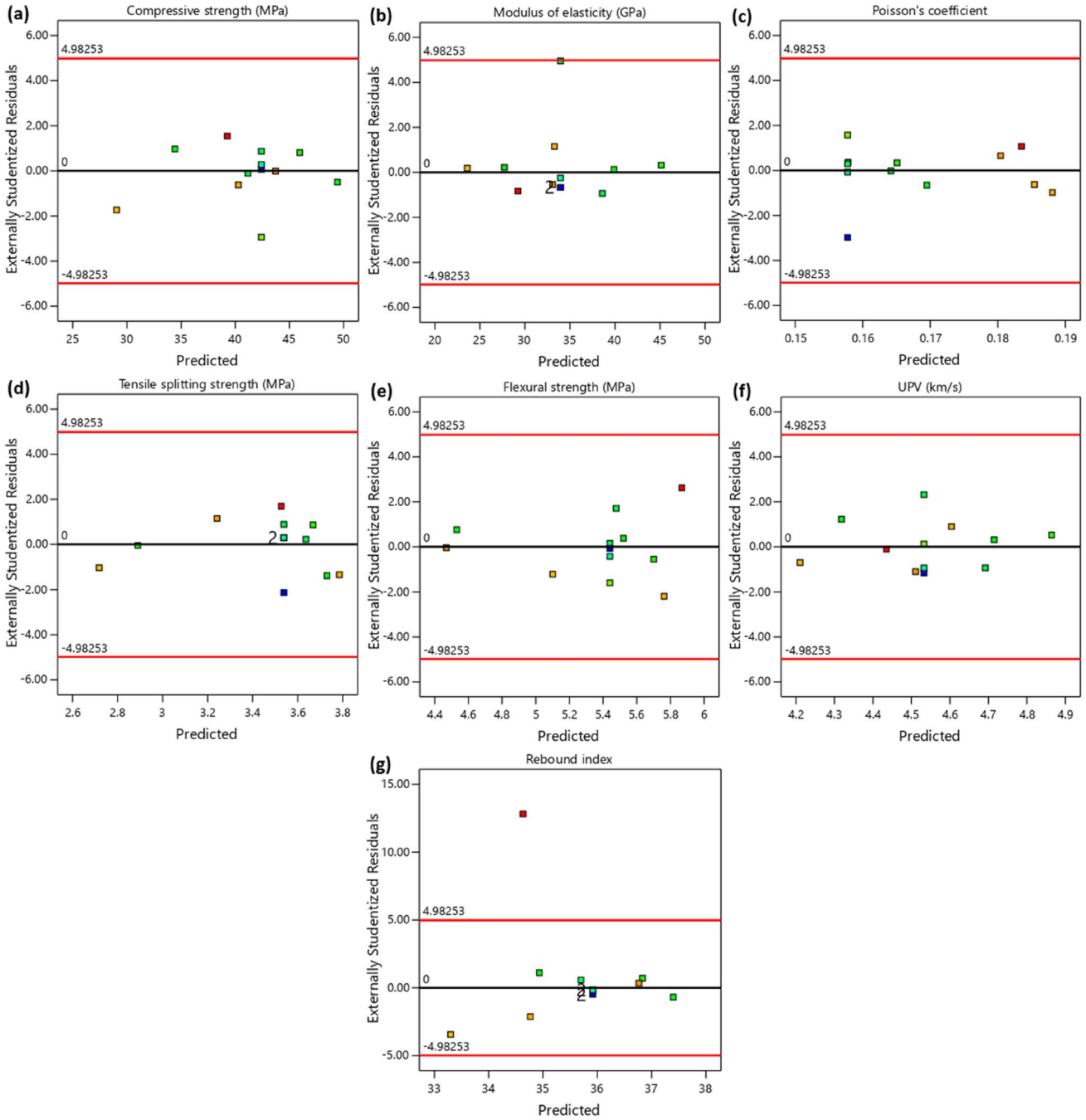

Fig. 3 Comparison between residuals and predicted values for optimum RSM models ($\alpha = \pm 1$): (a) compressive strength; (b) modulus of elasticity; (c) Poisson's coefficient; (d) tensile splitting strength; (e) flexural strength; (f) UPV; (g) rebound index

that the models developed for an α value of ± 1 were also adequate regarding the distribution of residuals, since in all cases it was random when compared to the predicted values of the properties, as can be observed in Fig. 3.

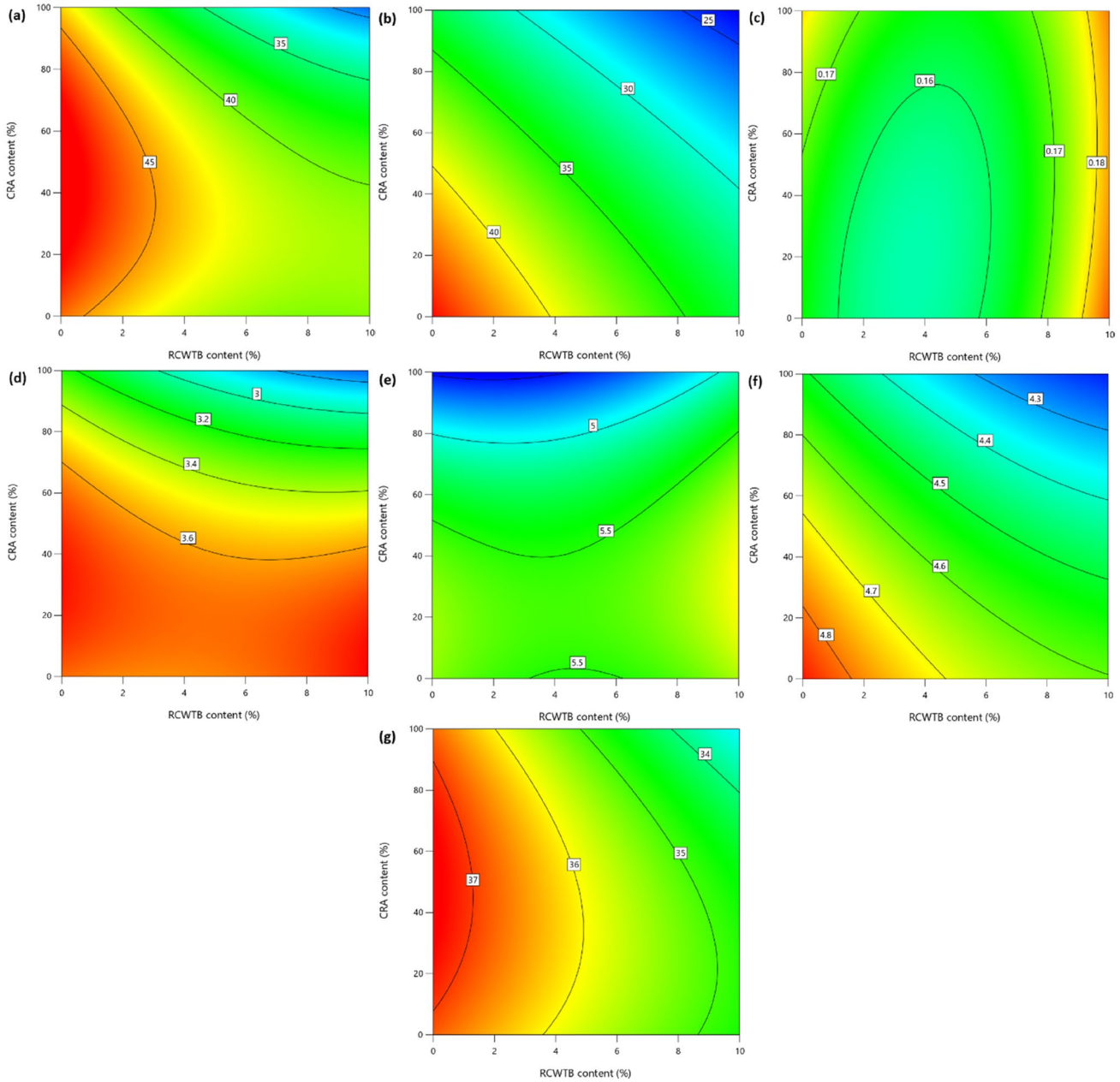

Fig. 4 Contour plots of optimum RSM models ($\alpha = \pm 1$) (red colors indicate high values of the property and blue colors mean low values): (a) compressive strength (MPa); (b) modulus of elasticity (GPa); (c) Poisson's coefficient (dimensionless); (d) tensile splitting strength (MPa); (e) flexural strength (MPa); (f) UPV (km/s); (g) rebound index (dimensionless)

4.3 Model analysis

4.3.1 Directions of maximum variation (gradients)

Figure 4 shows the contour plots of the optimum RSM models ($\alpha = \pm 1$), from which the directions of maximum variation (gradients) were identified. To define them, a two-dimensional Cartesian coordinate system was used, the x-axis indicating the RCWTB content (unit vector $\boldsymbol{i}$) and the y-axis the CRA amount (unit vector $\boldsymbol{j}$).

- The gradient of modulus of elasticity was approximately the vector $+\boldsymbol{i}+\boldsymbol{j}$, this property proportionally decreasing with the content of both residues. Compressive strength and tensile splitting strength also had this gradient for high contents of both wastes, since compressive strength did not depend on the CRA amount for low RCWTB contents (vector $+\boldsymbol{i}$ as gradient), while tensile splitting strength was not conditioned by RCWTB for low CRA amounts (vector $+\boldsymbol{j}$ as gradient).
- Poisson's coefficient and flexural strength were strongly conditioned by the stitching effect of the GFRP fibers and their interaction with the CRA content [22]. Therefore, they did not present constant gradients throughout the entire study space. Thus, Poisson's coefficient had as gradients the vectors $-\boldsymbol{i}+\boldsymbol{j}$ and $+\boldsymbol{i}$ for RCWTB contents lower and higher than 4%, respectively. The gradients for flexural strength were the vectors $+\boldsymbol{j}$ and $-\boldsymbol{j}$, 30% CRA being the frontier between them.
- NDT properties had constant gradients in the whole study space, the vector $+\boldsymbol{i}+\boldsymbol{j}$ for UPV, being affected by both wastes, and the vector $+\boldsymbol{i}$ for rebound index, as it was mainly affected by RCWTB.

UPV and modulus of elasticity of concrete exhibited identical gradients when adding both residues, suggesting a remarkable relationship between them, as stated in scientific literature [41, 42]. Compressive strength and tensile splitting strength also shared the same gradient when adding high waste contents. The gradient of rebound index only coincided with that of compressive strength for low RCWTB contents and with that of Poisson's coefficient from 4% RCWTB.

4.3.2 Maximum/minimum points

Figure 5 depicts the contents of CRA and RCWTB for which each property reached its maximum and minimum values in the study space. All these contents were determined through the optimum RSM models ($\alpha = \pm 1$), always choosing the waste combinations with the highest desirability [45, 51].

In relation to maximum points (Fig. 5a), only an exact coincidence was found between the UPV and the modulus of elasticity, which reached their maximum values for the same waste contents, showing their inherent

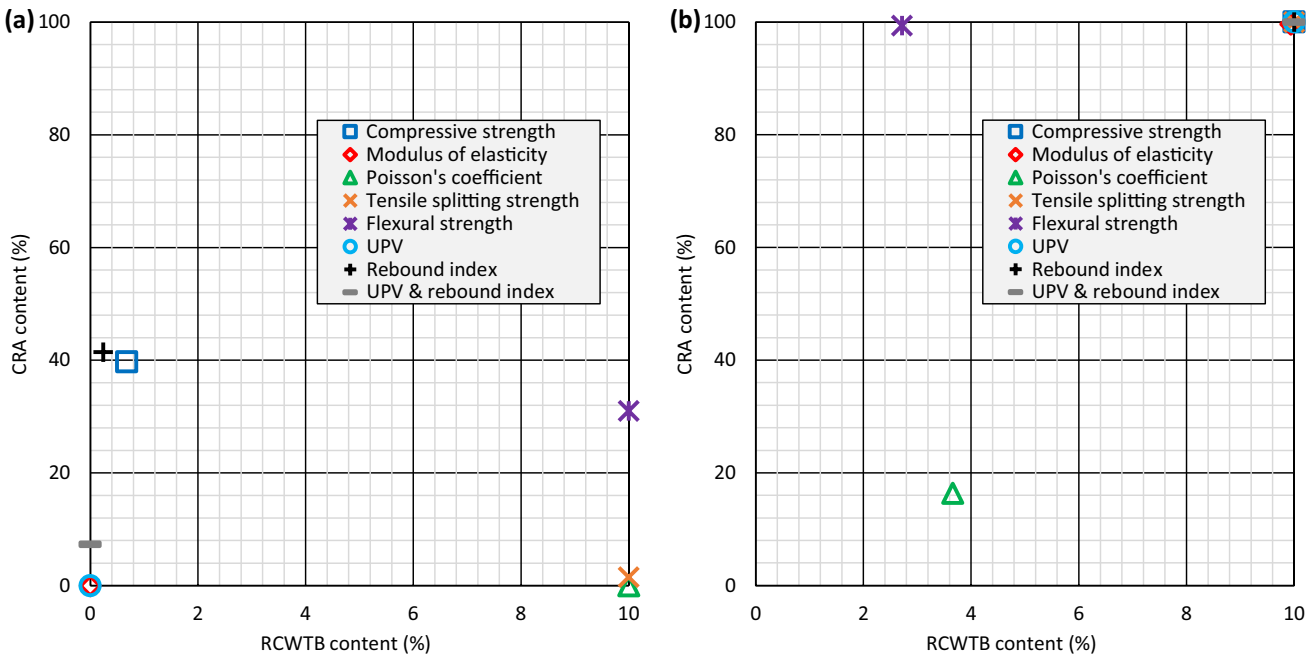

Fig. 5 Waste contents of the maximum and minimum values of the properties according to optimum RSM models ($\alpha = \pm 1$): (a) maximum points; (b) minimum points

relationship [40, 41]. Furthermore, the CRA content for which maximum UPV was obtained practically coincided with that of maximum Poisson's coefficient and maximum tensile splitting strength, while its RCWTB amount almost matched that of maximum compressive strength. On the other hand, the waste contents of maximum rebound index were almost the same as those of maximum compressive strength, while its RCWTB content practically matched that of maximum modulus of elasticity. UPV was closely related to a higher number of mechanical properties in terms of maximum points than rebound index. The simultaneous consideration of both NDT properties did not improve the accuracy yielded through only one NDT property. Finally, it should be noted that the contents of CRA and RCWTB for which maximum flexural strength was achieved were not close to those of any combination of NDT properties due to the dependence of this mechanical property on the GFRP fibers' stitching effect contained in the RCWTB [21].

In relation to the minimum points (Fig. 5b), they were reached for 100% CRA and 10% RCWTB for compressive strength, modulus of elasticity, tensile splitting strength, UPV and rebound index. Therefore, these three mechanical properties exhibited a clear relationship with both UPV and rebound index in terms of minimum points. The stitching of the cementitious matrix by the GFRP fibers affected Poisson's coefficient and flexural strength, which caused both mechanical properties to not experience as noticeable a decrease as the others as the waste contents increased [29]. Thus, the waste amounts corresponding to the minimum NDT properties were far from those that led to the minimum values of these mechanical properties.

5 Results and discussion: regression analysis

5.1 Overview

From the analysis of the directions of maximum variation and maximum/minimum points performed through RSM, it was found that UPV and modulus of elasticity followed the same trends of variation when both wastes were added. Compressive strength and tensile splitting strength also exhibited similar trends of variation to those of UPV when high waste contents were included. Regarding the rebound index, its trends coincided with those of compressive strength and Poisson's ratio, but only for certain RCWTB contents.

In order to verify these aspects from a regression approach to then define adequate estimations of the mechanical properties through NDT, a correlation analysis was first performed to approach the relationship between mechanical and NDT properties [40]. Subsequently, a regression analysis was conducted, thus expressing each mechanical property as a function of one or two NDT properties. By means of simple regression and linear multiple regression, those mechanical properties of concrete containing CRA and RCWTB that could be estimated by NDT were established, and the basis to develop non-linear multiple regression models for an optimal prediction of such mechanical properties was established. All these analyses were performed using Statgraphics software [52] accounting for the results of the four replicates performed with the central combination of residues (50% CRA and 5% RCWTB) for wider generalization [29].

5.2 Analysis of correlations

Correlations are commonly used to assess the validity of NDT to approach the mechanical behavior of concrete with varied compositions [37, 42]. These correlations, expressed as absolute values between 0 and 1, quantify the intensity of the relationship between two variables. The higher the value, the stronger the relationship. In addition, the sign indicates whether the relationship between variables is direct (positive sign, both variables increase or decrease simultaneously) or inverse (negative sign, one variable increases while the other decreases or vice versa). In this research, Pearson's correlations, which show a linear relationship, and Spearman's correlations, which detail if the relationship is monotonic, *i.e.*, if the rate of variation of the variables is not the same, were considered. The correlations between mechanical and NDT properties are detailed in Fig. 6.

 https://doi.org/10.1007/s43452-026-01442-4

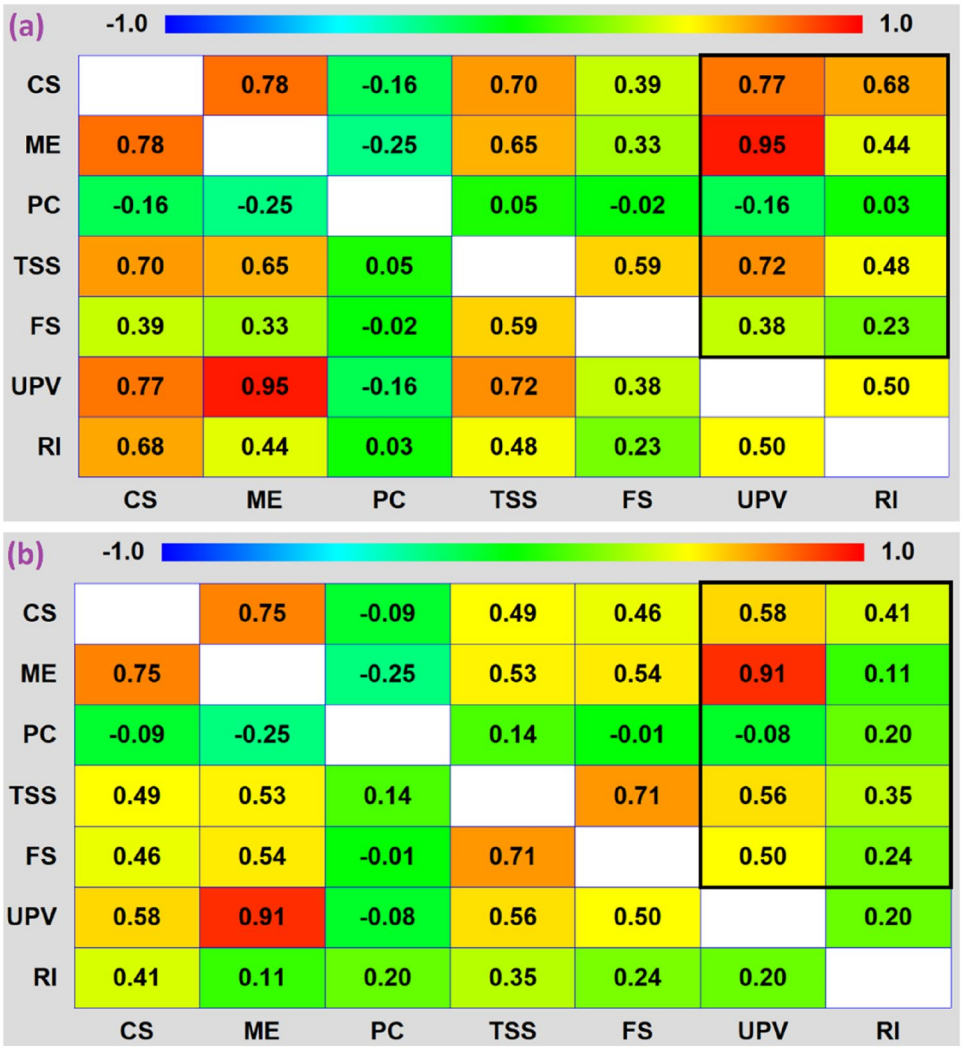

Fig. 6 Correlations: (a) Pearson; (b) Spearman. Correlations between mechanical properties and NDT framed in black. Legend: *CS* compressive strength, *ME* modulus of elasticity, *PC* Poisson's coefficient, *TSS* tensile splitting strength, *FS* flexural strength, *UPV* ultrasonic pulse velocity, *RI* rebound index

Correlations showed that the relationship between mechanical properties and NDT were mostly linear (higher Pearson's correlations), thus not requiring high powers to obtain an adequate estimation precision by regression [53], and more intense with UPV, since it was the NDT property that exhibited less variability [38]. The exception was flexural strength, which presented higher Spearman's correlations due to the stitching of the cementitious matrix by the GFRP fibers and its different effect with each CRA content [24]. Such stitching effect was enhanced when combined with some specific CRA contents, especially at 50% CRA. Analyzing each mechanical property separately, modulus of elasticity showed the highest Pearson's correlation, 0.95 with UPV, as usually reported in the literature [41]. Compressive strength and tensile splitting strength yielded Pearson's correlations of around 0.75 with UPV. Furthermore, compressive strength showed a Spearman's correlation with the rebound index of 0.68. These values were indicative that, in principle, regression models could be successfully developed to accurately estimate these mechanical properties using NDT [40]. Finally, sufficiently low correlations were not obtained for Poisson's coefficient and flexural strength in all cases to be able to state with full certainty that their estimation could not be successfully performed [53].

Table 6 Formulation of simple-regression models

Mechanical property	UPV			Rebound index		
	Type	*A*	*B*	Type	*A*	*B*
Compressive strength	Squared-root reciprocal[1]	15.9208	-43.2059	Double reciprocal	-0.0426	2.3944
Modulus of elasticity	Squared-root reciprocal[1]	17.7525	-54.0105	Double reciprocal	-0.0256	1.9741
Poisson's coefficient	Squared-root reciprocal[1]	0.3292	0.3711	Double reciprocal	5.7043	8.6057
Tensile splitting strength	Double reciprocal[2]	-0.4347	3.3044	Double reciprocal	-0.1250	14.9119
Flexural strength	Double reciprocal[2]	-0.0113	0.9010	Double reciprocal	0.1140	2.6175

[1]Model type *"squared-root reciprocal"* corresponds to Eq. (2)

[2]Model type *"double reciprocal"* matches Eq. (3)

5.3 Simple regression

Simple regression was used to evaluate whether each mechanical property could be estimated from a single NDT property. A R^2 maximization process yielded the most accurate estimates possible, the best models being always of a reciprocal nature: *"squared-root reciprocal"* models, Eq. (2), or *"double reciprocal"* models, Eq. (3). In these equations, *Pm* is the mechanical property (compressive strength, in MPa; modulus of elasticity, in GPa; Poisson's coefficient, dimensionless; tensile splitting strength, in MPa; or flexural strength, in MPa); *NDTp* is the NDT property considered (UPV, in km/s; or rebound index, dimensionless); and *A* and *B* are least-squares fit coefficients. Table 6 lists the most accurate model type for each combination of mechanical and NDT properties, as well as the values of the least-squares coefficients. All the models were of a *"double reciprocal"* type, except for the models estimating the compression-related properties through UPV. The relationship of UPV with the mechanical properties was conditioned by the type of stress applied, UPV usually showing a closer relationship with the compression-related properties [54], as shown in research conducted on concrete with CRA [38] and other alternative raw materials [42].

$$Pm = \left(A + \frac{B}{NDTp}\right)^2 \tag{2}$$

$$Pm = \frac{1}{A + \frac{B}{NDTp}} \tag{3}$$

Figure 7 shows the comparison between the experimental values of the mechanical properties and those estimated through simple-regression models. In addition, the accuracy analysis performed through deviation calculations is detailed in Table 7. Comparing the accuracy reached with both NDT properties, UPV always yielded better results, since the mean deviation (mean of the absolute values of the percentage differences between the estimated and experimental values) for all the properties never exceeded 7.5% when using it. Moreover, UPV estimated at least 75% of the experimental values with an accuracy of ± 10% regardless of the mechanical property. All this was because UPV exhibited clear trends when adding both wastes (Fig. 2a) [40], unlike the rebound index (Fig. 2b), which led to mean deviations of up to 11.0%. Evaluating the performance of the mechanical properties, modulus of elasticity was the most accurately estimated property through UPV, verifying all the trends discussed in the literature [53, 54]. The adhered mortar present in CRA and the weak particles in RCWTB weakened ITZ and increased the porosity of the cementitious matrix [4, 47, 48], being this effect more relevant regarding tensile splitting strength than the actual stitching by the GFRP fibers also contained in RCWTB. Thus, tensile splitting strength was also well adjusted by UPV, as this NDT property fundamentally reflects the characteristics of the cementitious matrix [42]. Flexural strength was accurately estimated through both NDT properties, being the only mechanical property adjusted with proper accuracy through rebound index. Finally, compressive strength and Poisson's coefficient were predicted with a mean deviation of 7.0% through UPV, 75% of their experimental results being estimated with an accuracy of ± 10%.

 https://doi.org/10.1007/s43452-026-01442-4

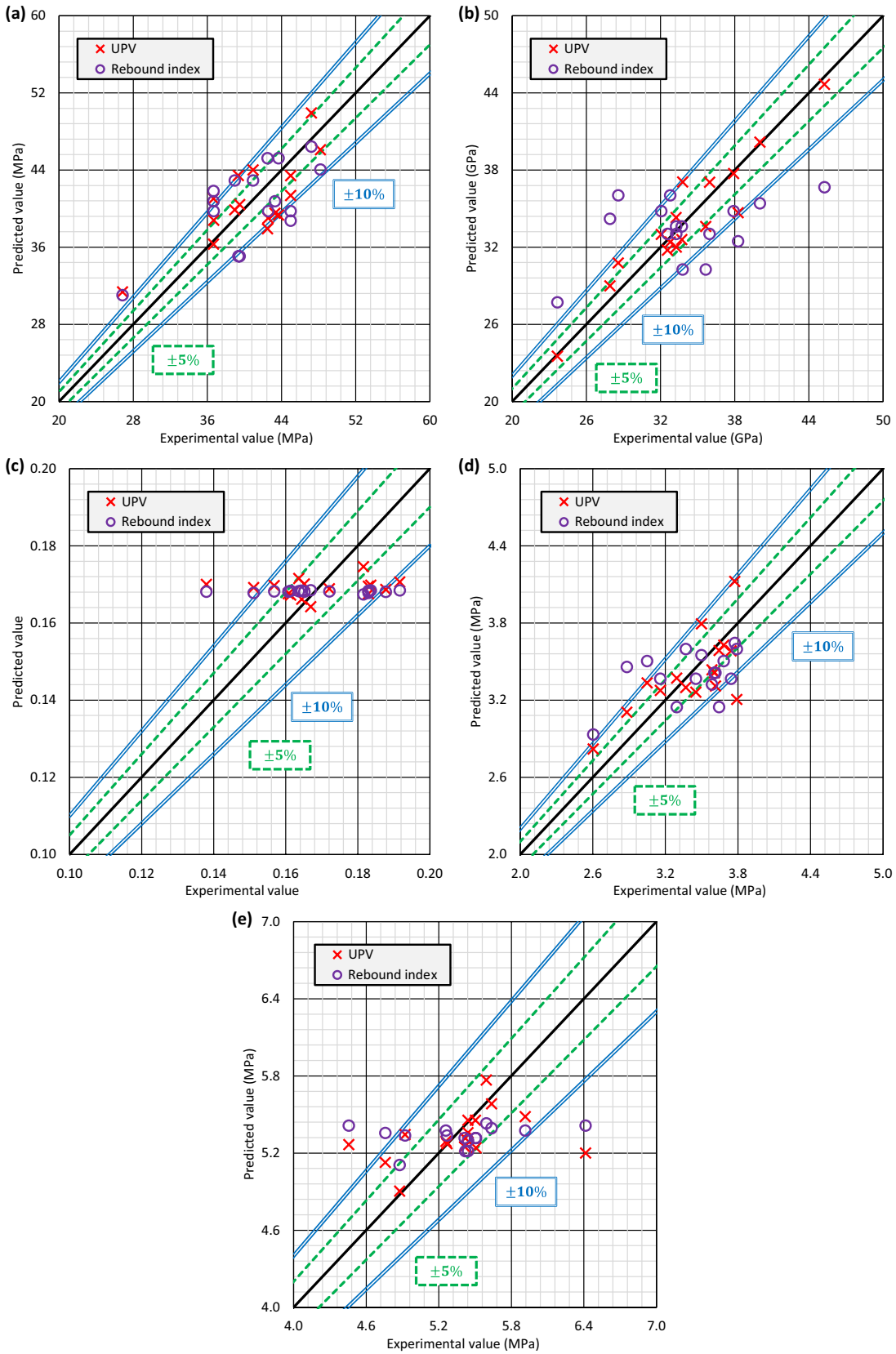

Fig. 7 Comparison between experimental and predicted values through simple-regression models: (a) compressive strength; (b) modulus of elasticity; (c) Poisson's coefficient; (d) tensile splitting strength; (e) flexural strength

Table 7 Accuracy analysis of simple-regression models

Mechanical property	UPV			Rebound index		
	Mean deviation (%)	5%-accuracy predictions (%)	10%-accuracy predictions (%)	Mean deviation (%)	5%-accuracy predictions (%)	10%-accuracy predictions (%)
Compressive strength	7.3	31.3	75.0	9.0	18.8	50.0
Modulus of elasticity	3.7	75.0	100.0	11.0	25.0	50.0
Poisson's coefficient	7.0	50.0	75.0	7.1	43.8	75.0
Tensile splitting strength	6.1	43.8	93.8	7.8	31.3	68.8
Flexural strength	4.9	68.8	87.5	6.4	68.8	81.3

Table 8 Goodness-of-fit indicators for simple-regression models

Mechanical property	UPV			Rebound index		
	R^2 (%)	Model p-value	Durbin-Watson p-value	R^2 (%)	Model p-value	Durbin-Watson p-value
Compressive strength	60.93	0.0004	0.7126	52.40	0.0015	0.5413
Modulus of elasticity	89.59	0.0000	0.1296	24.01	0.0540	0.2439
Poisson's coefficient	2.47	0.5607	0.0919	0.03	0.9450	0.1101
Tensile splitting strength	56.76	0.0008	0.4366	27.26	0.0380	0.4582
Flexural strength	17.54	0.1064	0.6636	3.49	0.4884	0.8545

Table 8 shows the goodness-of-fit indicators of simple-regression models. Analyzing first model significance, UPV-dependent models for Poisson's coefficient and flexural strength were not significant at a 95% confidence level (model p-values higher than 0.05). The models dependent on rebound index for these properties were also not significant, as well as the model for modulus of elasticity. Only the models for compressive strength and tensile splitting strength, regardless of the NDT property, and the UPV-dependent model for modulus of elasticity were valid. The accuracy yielded when estimating flexural strength (Table 7) was therefore trivial, not due to the existence of a clear dependence between it and the NDT properties [39]. In fact, it can be observed in Fig. 7e the absence of a clear relationship between the experimental and estimated values of this property, almost the same predicted value being obtained for all the experimental results. Addressing the proportion of experimental variance explained by the statistically significant models, the UPV-dependent model for modulus of elasticity was the only one that showed a high R^2 coefficient of approximately 90%. UPV led to R^2 coefficients of 55–60% for compressive strength and tensile splitting strength, valid but somewhat low according to usual statistical approaches [5]. Rebound index yielded the same performance for compressive strength, but it provided only an R^2 coefficient of about 27% for tensile splitting strength, which is clearly insufficient [5]. Multiple regression could be therefore a way to improve such dimension in terms of compressive strength [40]. Finally, all the statistically significant models had the necessary random distribution of residuals at a 95% confidence level to guarantee their suitability, since their Durbin-Watson p-value was always higher than 0.05.

The statistically significant simple-regression models are plotted in Fig. 8. These models were approximately linear in the ranges of study of the NDT properties (4.0–5.0 km/s for UPV and 30–40 units for rebound index) or showed slight concave curvatures. This was consistent with the correlation analysis, which revealed that Pearson's correlations had the highest values (Fig. 6), the relationships between variables being therefore fundamentally linear [53]. Furthermore, such representations also allowed verifying that UPV was the NDT property that always yielded a more precise estimation. In the UPV-dependent models for compressive strength (Fig. 8a), modulus of elasticity (Fig. 8c) and tensile splitting strength (Fig. 8d), the experimental results followed the model's trend. However, in the models dependent on the rebound index (Fig. 8b for compressive strength and Fig. 8e for tensile splitting strength) the experimental results were more like a point cloud, not following the trend established by the model so clearly, thus yielding lower R^2 coefficients for that NDT property (Table 8), and the model explaining worse experimental variability [39].

 https://doi.org/10.1007/s43452-026-01442-4

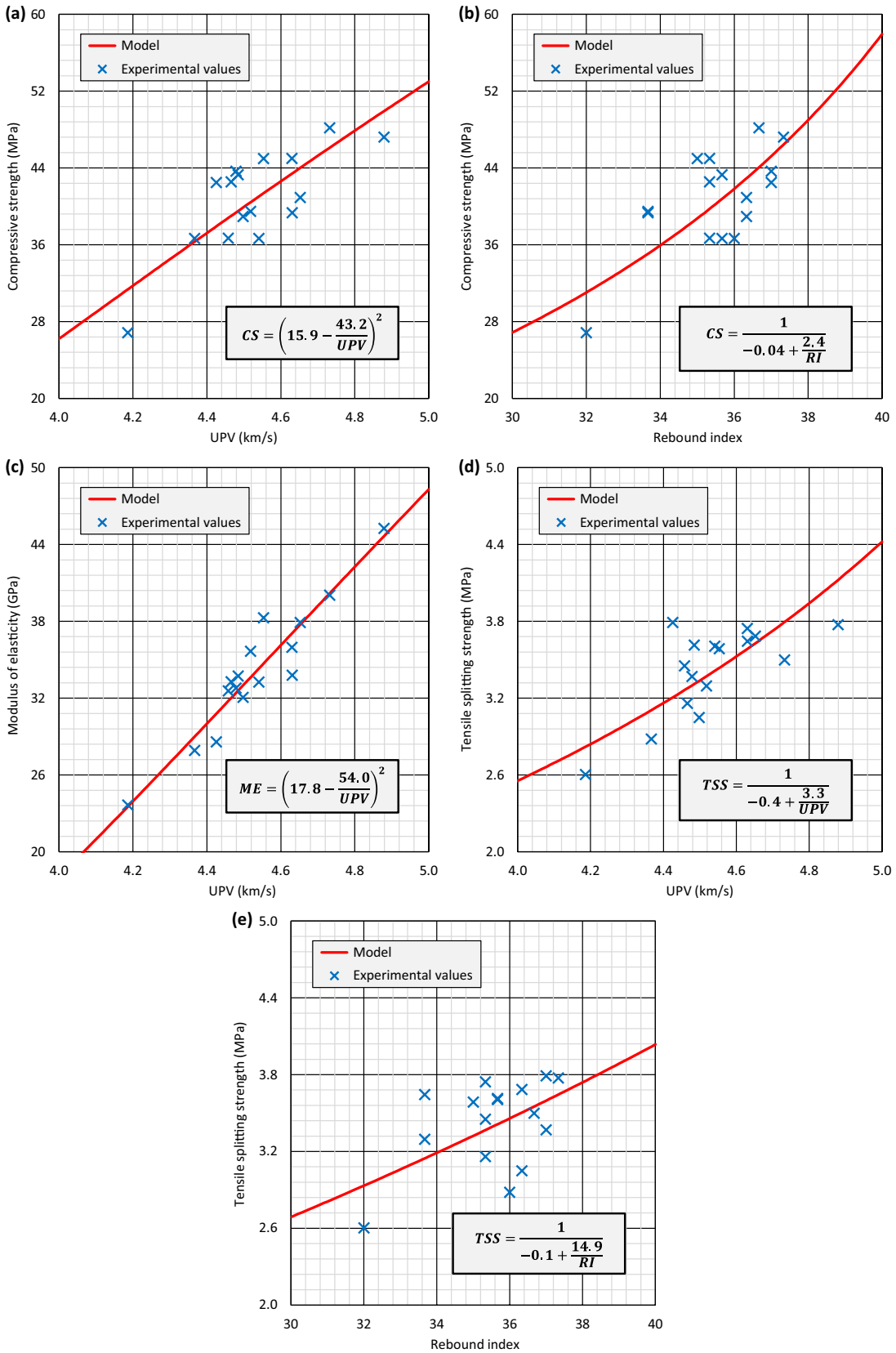

Fig. 8 Statistically significant simple-regression models: (a) compressive strength as a function of UPV; (b) compressive strength as a function of rebound index; (c) modulus of elasticity as a function of UPV; (d) tensile splitting strength as a function of UPV; (e) tensile splitting strength as a function of rebound index. Legend: *CS* compressive strength, *ME* modulus of elasticity, *TSS* tensile splitting strength, *UPV* ultrasonic pulse velocity, *RI* rebound index

Table 9 Significance *p*-values of the terms of the statistically significant simple-regression models

Mechanical property	UPV		Rebound index	
	Intercept (*A*)	Slope (*B*)	Intercept (*A*)	Slope (*B*)
Compressive strength	0.0000	0.0004	0.0269	0.0015
Modulus of elasticity	0.0000	0.0000	- *	
Tensile splitting strength	0.0231	0.0008	0.5072	0.0380

*The model for modulus of elasticity as a function of rebound index was not significant

Table 10 Formulation of linear multiple-regression models

Mechanical property	*C*	*D*	*E*
Compressive strength	-95.8603	18.8484	1.4431
Modulus of elasticity	-102.2160	31.1761	-0.1409
Poisson's coefficient	0.2148	-0.0216	0.0015
Tensile splitting strength	-4.3193	1.4076	0.0384
Flexural strength	-0.0440	1.0501	0.0183

Finally, it should be noted from Table 9 that both the intercepts, *A* in Eq. (2) and Eq. (3), and the slopes, *B* in Eq. (2) and Eq. (3), of the statistically significant simple-regression models were significant at a 95% confidence level (*p*-values lower than 0.05), contributing effectively to improved estimation accuracy. The only exception was the model dependent on the rebound index for tensile splitting strength, whose intercept was not significant and only increased the complexity of the model without improving the estimation accuracy, so it could be safely eliminated without affecting model's quality [5].

5.4 Linear multiple regression

In view of the simple-regression results, an analysis through linear multiple regression was conducted. The aim was to determine whether this statistical methodology enabled to improve the estimation accuracy for compressive strength and tensile splitting strength, and to achieve statistically significant models for Poisson's coefficient and flexural strength. Thus, each mechanical property was expressed as a linear combination of the first powers of both NDT properties, as shown in Eq. (4). In this equation, *Pm* is the mechanical property (compressive strength, in MPa; modulus of elasticity, in GPa; Poisson's coefficient, dimensionless; tensile splitting strength, in MPa; or flexural strength, in MPa); *UPV* is the UPV value in km/s; *RI* is the dimensionless value of rebound index; and *C*, *D* and *E* are least-squares adjustment coefficients. Table 10 lists the values of these coefficients, which at first glance did not reveal a greater influence of one NDT property than another in accordance with the findings of other research [40, 55].

$$Pm = C + D \cdot UPV + E \cdot RI \tag{4}$$

As for simple regression, estimation accuracy was first analyzed. For this purpose, the comparison between experimental and predicted values is shown in Fig. 9, while the first columns of Table 11 provide a detailed analysis of deviations. Comparing the mechanical properties with each other, the trends found in simple regression when using UPV as the independent variable were maintained. Therefore, modulus of elasticity was the most accurately estimated mechanical property (mean deviation of 3.6%), followed by flexural strength, compressive strength, tensile splitting strength and Poisson's coefficient, which showed a high mean deviation of 7.1%. It seems clear from such situation that the linear multiple-regression models mainly depended on UPV, as it was the NDT property that exhibited the least experimental variability [38] and that followed trends closer to those of mechanical properties when both wastes were added according to the RSM analysis [51]. Another aspect worth noting is that compressive strength was the only mechanical property whose estimation accuracy was improved when both NDT measurements were simultaneously considered. Thus, its mean deviation and its percentage of experimental results estimated with an accuracy of ± 10% when using the UPV-dependent simple-regression

 https://doi.org/10.1007/s43452-026-01442-4

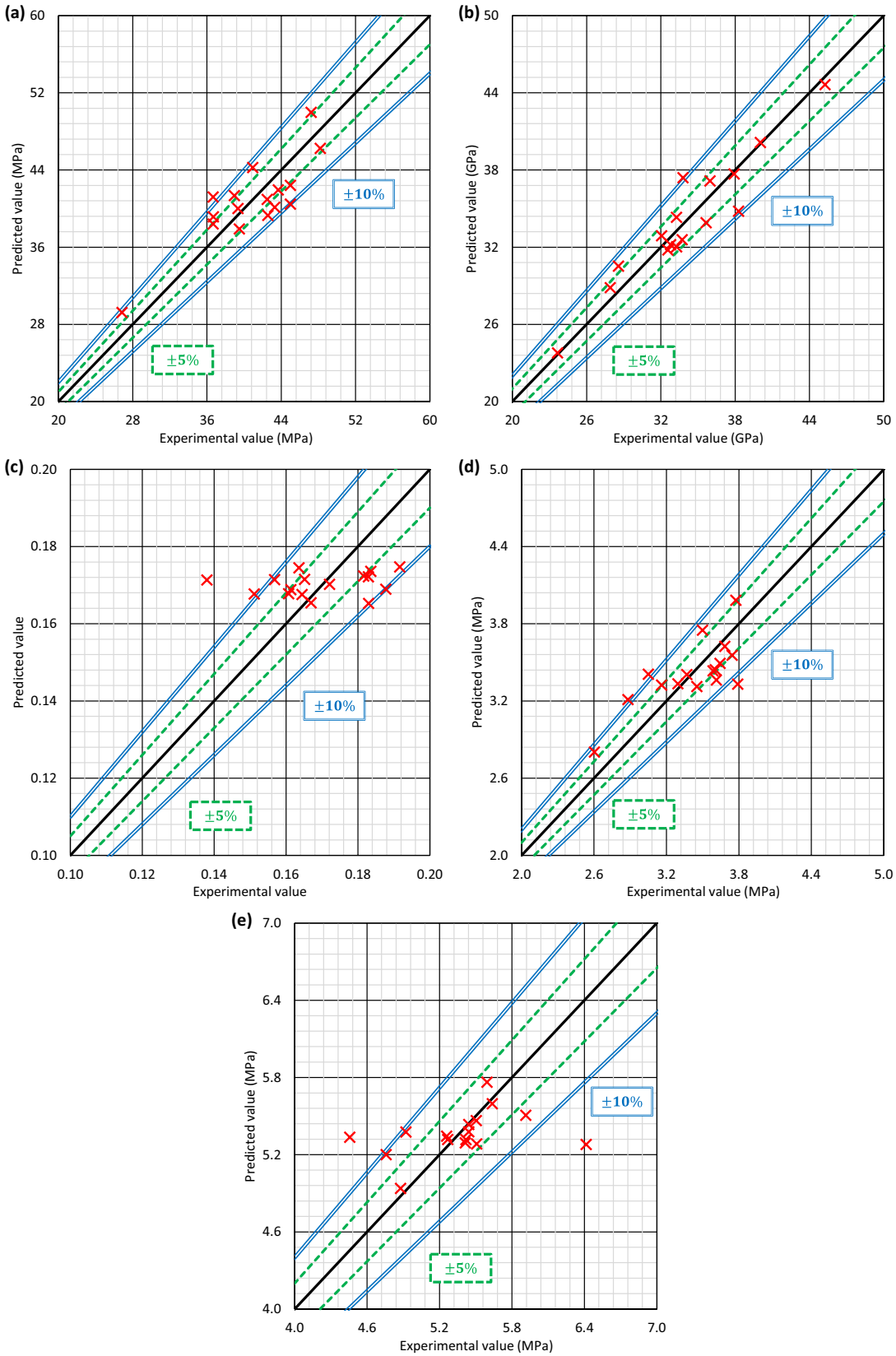

Fig. 9 Comparison between experimental and predicted values through linear multiple-regression models: (a) compressive strength; (b) modulus of elasticity; (c) Poisson's coefficient; (d) tensile splitting strength; (e) flexural strength

Table 11 Accuracy analysis and goodness-of-fit indicators of linear multiple-regression models

Mechanical property	Mean deviation (%)	5%-accuracy predictions (%)	10%-accuracy predictions (%)	R^2 (%)	Model p-value	Durbin-Watson p-value
Compressive strength	6.3	37.5	87.5	70.41	0.0004	0.6268
Modulus of elasticity	3.6	81.3	93.8	89.51	0.0000	0.1547
Poisson's coefficient	7.1	37.5	81.3	4.04	0.7647	0.0573
Tensile splitting strength	5.9	43.8	81.3	53.88	0.0065	0.3185
Flexural strength	5.0	68.8	87.5	14.87	0.3511	0.7017

model were 7.3% and 75.0%, respectively. These values were improved to 6.3% and 87.5%, respectively, by linear multiple regression. It is thought that combining UPV and rebound index in the estimation model joined the assessment of the cementitious-matrix characteristics provided by UPV [31] with the evaluation through rebound index of the beneficial confinement effect under compression loads that the GFRP fibers within RCWTB could exert [13].

The goodness-of-fit indicators for the linear multiple-regression models are shown in the last columns of Table 11. As for simple regression, the models developed for Poisson's coefficient and flexural strength were not significant at a confidence level of 95%, their model p-values not exceeding the limit value of 0.05. Once again, there was no clear relationship between the experimental and predicted values [5], evident by the scattering cloud appearance of Fig. 9c for Poisson's coefficient and Fig. 9e for flexural strength. The adequate prediction accuracy yielded for flexural strength (Table 11) was therefore trivial, the NDT properties considered in this research not allowing to adequately approach through multiple regression the stitching effect of the cementitious matrix by the GFRP fibers contained in RCWTB, which in turn notably conditioned this mechanical property [21, 29]. On the other hand, among all the statistically significant linear multiple-regression models (compressive strength, modulus of elasticity and tensile splitting strength), only the model for compressive strength improved the R^2 coefficient of the corresponding UPV-dependent simple-regression model (60.93% vs. 71.41%) and, consequently, the quality of the regression adjustment [39]. For the other mechanical properties, the combination of UPV with rebound index led to models that adequately described their variation trends when adding both wastes, but did not improve the fitting quality yielded by exclusively using UPV. Finally, all the models presented a Durbin-Watson p-value higher than 0.05, so all of them had the necessary random distribution of residuals at a confidence level of 95% to guarantee their validity.

The reduced contribution of rebound index to the improvement of the estimation quality of mechanical properties was verified through the graphical representation of the statistically significant linear multiple-regression models (Fig. 10). The contour plot of the model for compressive strength (Fig. 10a) showed a series of parallel bands that formed approximately a 45° angle with both axes, both NDT properties clearly conditioning the estimated value of this strength [45]. However, these bands were approximately parallel to the rebound-index axis for the models for modulus of elasticity (Fig. 10b) and tensile splitting strength (Fig. 10c), which showed that the estimated value of these mechanical properties depended almost exclusively on UPV [51]. The analysis of the significance of the terms of these models (Table 12) yielded the same conclusions. While the UPV-dependent term, D in Eq. (4), was always significant by presenting a p-value lower than 0.05, the term dependent on rebound index, E in Eq. (4), was only significant for compressive strength. This analysis also showed that the intercept, C in Eq. (4), was not significant in the model for tensile splitting strength, so it could be removed without worsening model's quality [5].

 https://doi.org/10.1007/s43452-026-01442-4

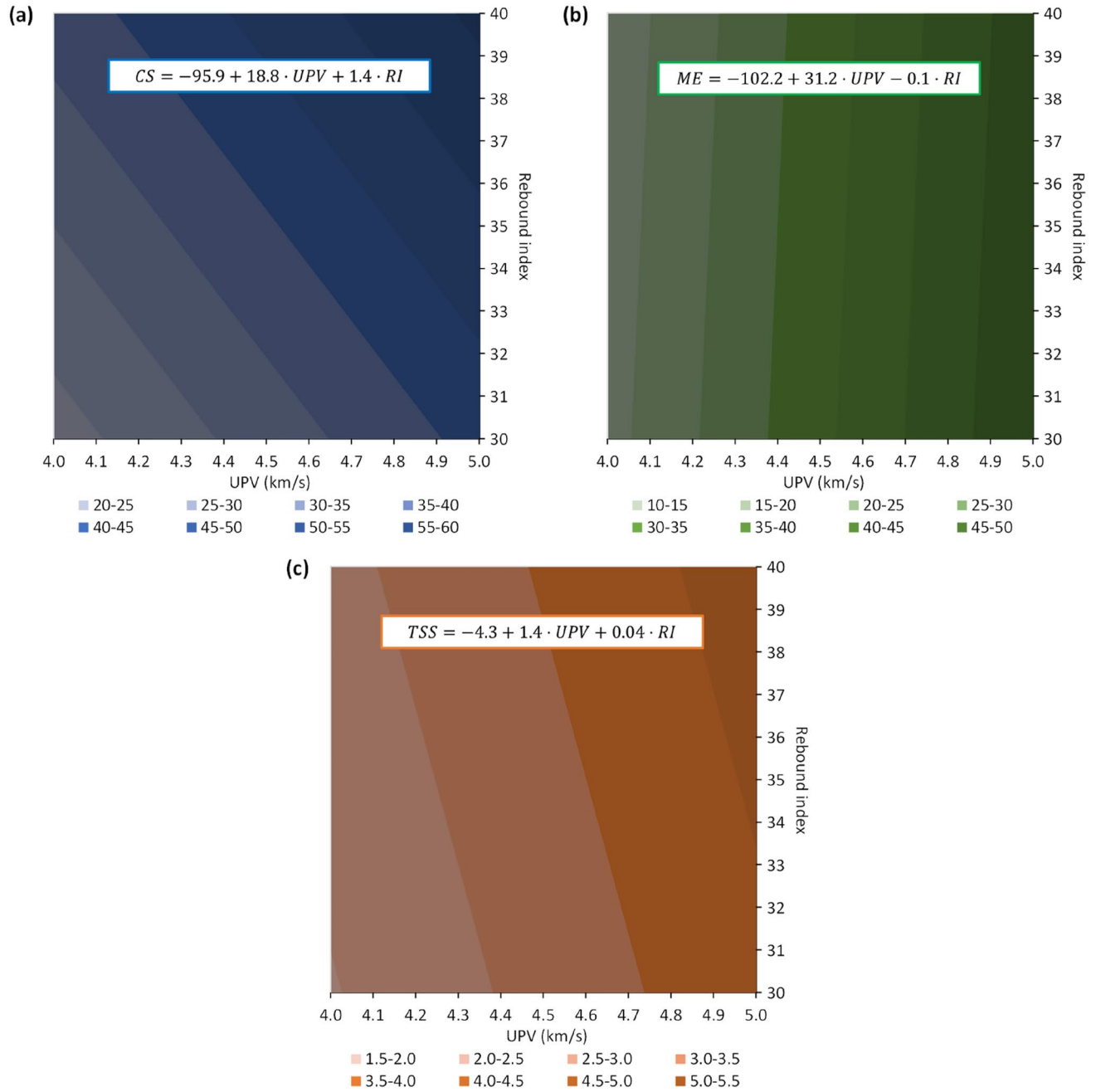

Fig. 10 Contour plots of the statistically significant linear multiple-regression models: (a) compressive strength (MPa); (b) modulus of elasticity (GPa); (c) tensile splitting strength (MPa). Legend: *CS* compressive strength, *ME* modulus of elasticity, *TSS* tensile splitting strength, *UPV* ultrasonic pulse velocity, *RI* rebound index

Table 12 Significance *p*-values of the terms of the valid linear multiple-regression models

Mechanical property	Intercept (C)	UPV slope (D)	Rebound-index slope (E)
Compressive strength	0.0018	0.0060	0.0411
Modulus of elasticity	0.0000	0.0000	0.7096
Tensile splitting strength	0.0534	0.0111	0.4789

5.5 Non-linear multiple regression

5.5.1 Model definition

From the simple-regression and linear multiple-regression analyses, the following conclusions were reached for each mechanical property:

- The highest accuracy and goodness of fit for the estimation of compressive strength was obtained by combining UPV and rebound index in the prediction model.
- The simplest way to estimate modulus of elasticity and tensile splitting strength was through exclusively UPV, since rebound index did not allow improving prediction quality.
- Poisson's coefficient and flexural strength did not show a clear relationship with any NDT property, so no significant models could be developed to estimate these properties in a non-trivial way.

Based on these aspects, models through non-linear multiple regression were developed to estimate compressive strength, modulus of elasticity and tensile splitting strength as accurately as possible. For this purpose, the values of the adjustment coefficients were iteratively determined by least squares using the Marquadt method [56]. By applying this method, the number of iterations was limited to those necessary to achieve an error in these coefficients of 0.1%, thus avoiding excessive computational cost [55]. Expressions were obtained to approach the mean and minimum expected values at a confidence level of 95%:

- The optimal model for estimating compressive strength is shown in Eq. (5) for the mean expected value and Eq. (6) for the minimum expected value. This model incorporated two terms inversely dependent on the NDT properties, following the formulation of simple-regression models. An intercept and two terms dependent on the first powers of the NDT properties were incorporated to reflect the strong linear relationship of this mechanical property with them (Fig. 6), also found through linear multiple regression (Table 12).
- The model for modulus of elasticity is detailed in Eq. (7) and Eq. (8) regarding the mean and minimum expected values, respectively, which depended exclusively on UPV. This was exactly the simple regression model, as no improvement in goodness-of-fit and estimation accuracy was achieved by introducing any additional terms.
- Finally, the model for tensile splitting strength, shown in Eq. (9) for the expected mean value and Eq. (10) for the expected minimum value, was composed of a term following the formulation of the simple regression model as a function of UPV combined with a term dependent on the first power of this NDT measurement. An intercept not dependent on the NDT properties was not introduced because it was not significant, as noted in linear multiple regression (Table 12).

$$CS = 314.1 - 77.3 \cdot UPV - \frac{4529.3}{UPV^2} + 4.9 \cdot RI + \frac{4462.9}{RI} \tag{5}$$

$$CS = 803.1 - 97.6 \cdot UPV - \frac{5476.0}{UPV^2} - 0.2 \cdot RI - \frac{1815.9}{RI} \tag{6}$$

$$ME = \left(17.8 - \frac{54.0}{UPV}\right)^2 \tag{7}$$

$$ME = \left(17.5 - \frac{54.2}{UPV}\right)^2 \tag{8}$$

$$TSS = \frac{1}{\left(0.1 + \frac{0.3}{UPV}\right)^2} - 10.8 \cdot UPV \tag{9}$$

$$TSS = \frac{1}{\left(0.1 + \frac{0.4}{UPV}\right)^2} - 8.5 \cdot UPV \tag{10}$$

 https://doi.org/10.1007/s43452-026-01442-4

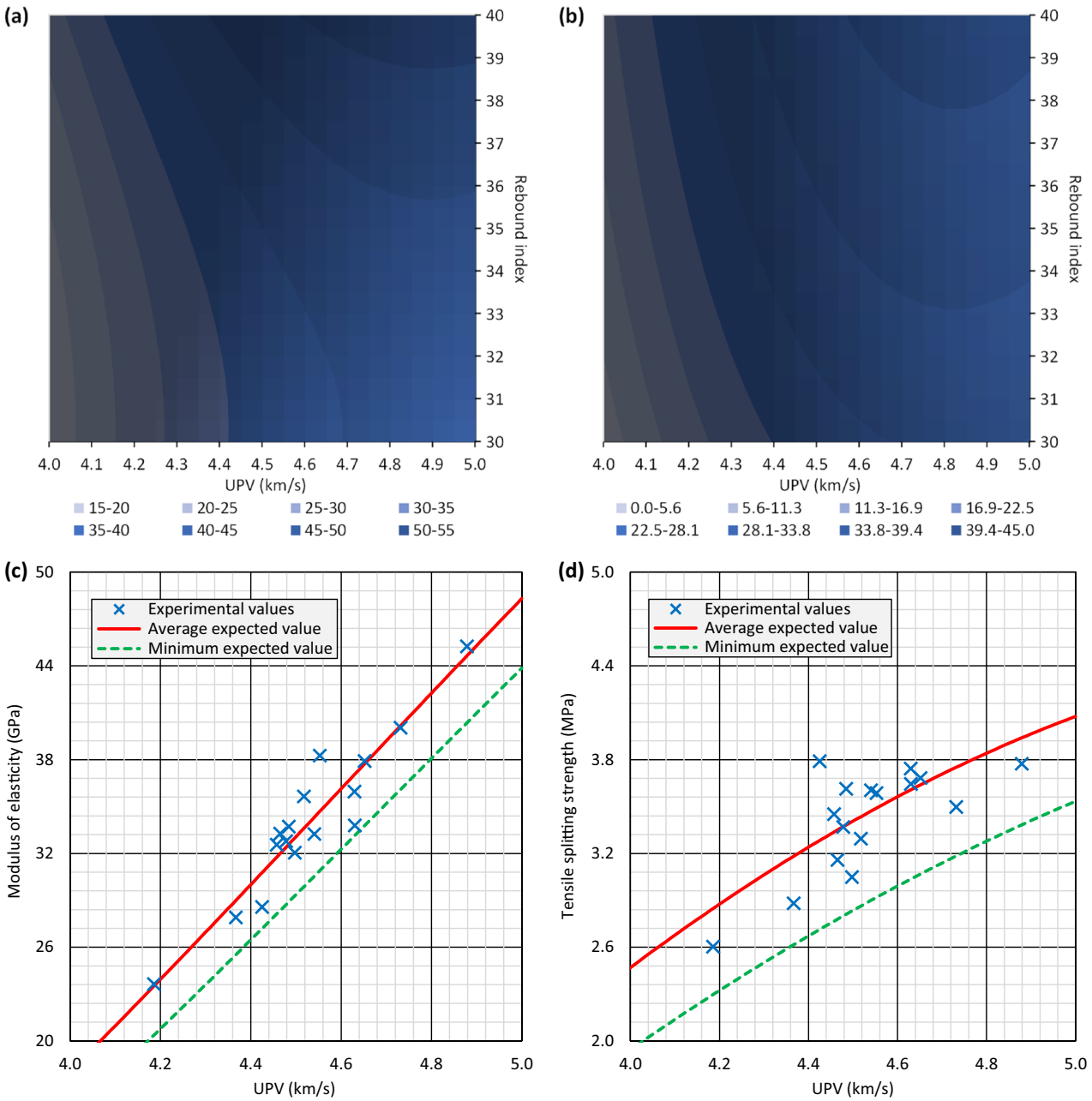

Fig. 11 Non-linear multiple-regression models: (a) mean expected value of compressive strength in MPa (contour plot); (b) minimum expected value of compressive strength in MPa (contour plot); (c) modulus of elasticity; (d) tensile splitting strength

Non-linear multiple-regression models are shown in Fig. 11. The model for compressive strength depended on both UPV and rebound index, so it is represented as a contour plot. The models for modulus of elasticity and tensile splitting strength depended only on UPV, so they are represented two-dimensionally:

- For compressive strength (Fig. 11a and b), the model revealed an increase of estimated strength approximately proportional to UPV up to UPV values of 4.4 km/s, rebound index being almost irrelevant. However, the estimated strength depended on rebound index to a greater extent for UPV values higher than 4.4 km/s, the model

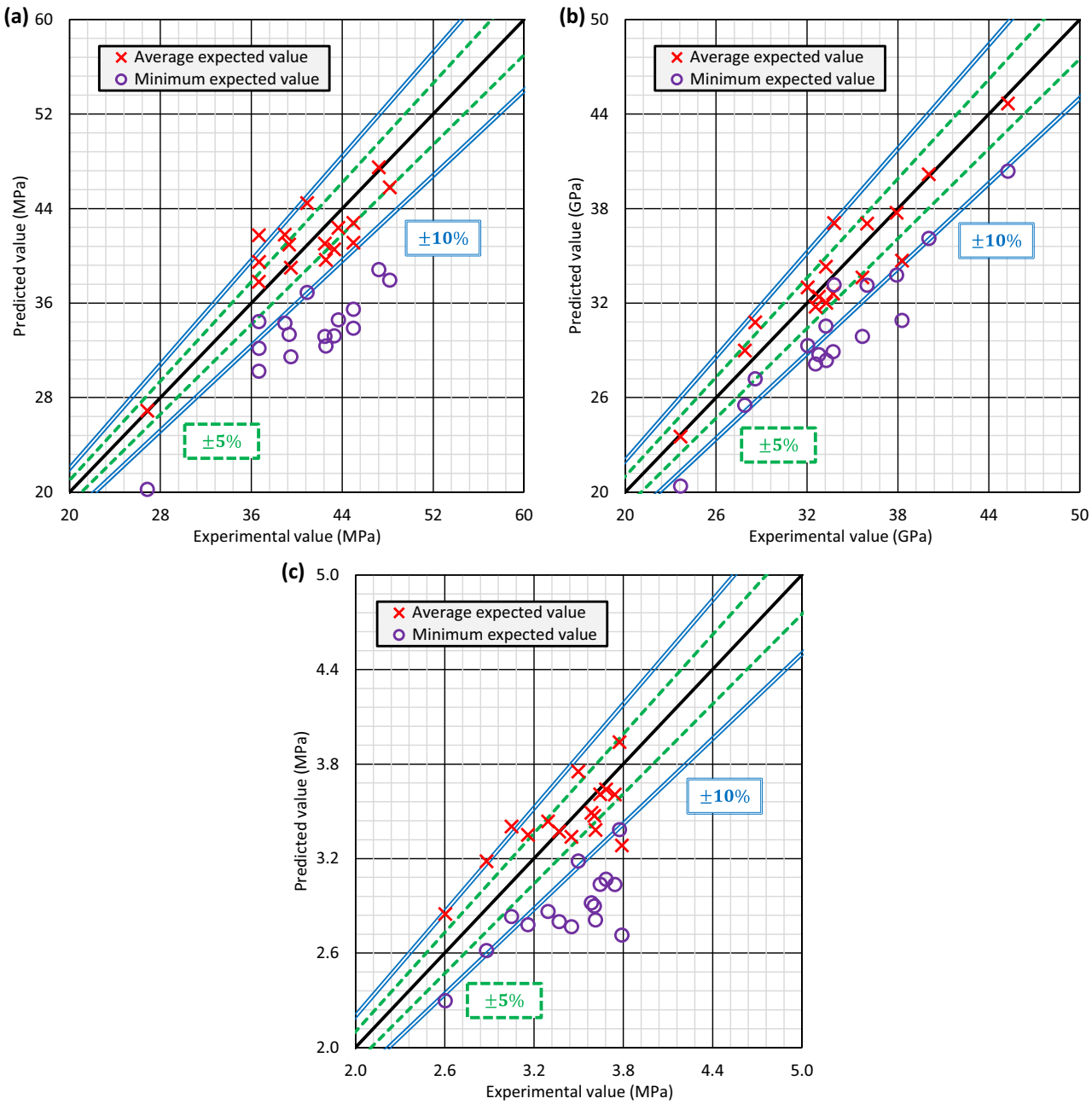

Fig. 12 Comparison between experimental and predicted values through non-linear multiple-regression models: (a) compressive strength; (b) modulus of elasticity; (c) tensile splitting strength

Table 13 Accuracy analysis and goodness-of-fit indicators of non-linear multiple-regression models

Mechanical property	Mean deviation (%)	5%-accuracy predictions (%)	10%-accuracy predictions (%)	R^2 (%)	Mean absolute error	Durbin-Watson statistic*
Compressive strength	5.3	56.3	93.8	74.36	2.1664	2.1388 (1.9351)
Modulus of elasticity	3.6	81.3	93.8	89.51	0.1067	1.5315 (1.3709)
Tensile splitting strength	5.6	56.3	81.3	64.06	0.1846	2.0138 (1.5386)

*The minimum value of the Durbin-Watson statistic for absence of correlation between residuals in each case is shown in brackets

thus presenting a parabolic shape. For UPV values between 4.8 km/s and 5.0 km/s, the estimated strength depended almost exclusively on rebound index. This demonstrated the need of estimating compressive strength by considering both NDT measurements to properly describe the trends depicted by this mechanical property [40].

- The models for modulus of elasticity (Fig. 11c) and tensile splitting strength (Fig. 11d) exhibited an approximately linear shape in the study space, with a reduced curvature. These models effectively described both mechanical properties by fitting the trends of their experimental results. Non-linear multiple regression therefore validated previous findings such as those of the correlation analysis, (Fig. 6), showing a predominant linear relationship between these mechanical properties and UPV.

Figure 12 compares the experimental values of the mechanical properties with those estimated through non-linear multiple-regression models. In addition, the first columns of Table 13 depict the accuracy of the models through deviations. First, it should be noted that the minimum expected values were always lower than the experimental ones, providing the model in principle with an adequate safety margin [44]. Second, the models presented an adequate accuracy according to previous research [35, 53], with mean deviations of around 3–6%, improving the precision yielded through linear multiple regression, especially for compressive strength. In addition, around 80–90% of the experimental values were estimated with an accuracy of ± 10%. However, the estimation was better for compression-related properties, due to the stronger link of both NDT properties to the quality of the cementitious matrix, affected by CRA and the weak and deformable particles included in RCWTB [37, 47], than to the stitching effect of the GFRP fibers contained in RCWTB [42], which partially conditioned the trends exhibited by tensile splitting strength when RCWTB was added [21]. In particular, modulus of elasticity was the property that was most accurately estimated due to its close relationship with UPV [54], as this property is little dependent on the GFRP fibers because the strain in the elastic zone of concrete was not high enough for these fibers to work effectively [14]. Goodness-of-fit indicators, shown in the last columns of Table 13, reflected these same aspects, with the R^2 coefficient and the mean absolute error (average of the differences between the experimental and estimated values in absolute value) presenting the best results for modulus of elasticity, then for compressive strength and finally for tensile splitting strength. All the models presented a random distribution of residuals according to the Durbin-Watson statistic.

5.5.2 Safety factors

Apart from comparing the experimental and minimum expected values, the estimative safety of the optimal models obtained through non-linear multiple regression was determined by calculating the safety factors for the mean and minimum expected values [57]. The calculation of the safety factors followed these steps:

1. Each experimental result was divided by its corresponding mean and minimum expected values.

Table 14 Safety-factor evaluation for non-linear multiple-regression models

Mechanical property	Expected value	χ^2 test p-value	Saphiro-Wilk test p-value	Skewness Z-score test p-value	Mean (μ)	Standard deviation (σ)	Kolmogorov–Smirnov test p-value
Compressive strength	Mean	0.5341	0.6865	0.6386	1.0000	0.0631	0.9677
	Minimum	0.2757	0.1967	0.4102	1.2293	0.0821	0.6362
Modulus of elasticity	Mean	0.6890	0.9744	0.8580	1.0006	0.0483	0.9962
	Minimum	0.8343	0.9962	0.9235	1.1259	0.0553	0.9928
Tensile splitting strength	Mean	0.2757	0.4294	0.4664	0.9932	0.0690	0.9506
	Minimum	0.1866	0.2909	0.2935	1.1907	0.0833	0.9681

2. For each mechanical property and type of expected value, it was verified whether the set of results obtained through those divisions followed a normal distribution. For that, several hypothesis tests were considered: χ^2 test, which compares the frequencies of the data with those of a normal distribution; Saphiro-Wilk test, which evaluates the goodness-of-fit of the data to a normal distribution; and the Skewness Z-score test, which analyzes whether the frequencies of the data are symmetrical. A *p*-value greater than 0.05 was always indicative that the normality requirement was fulfilled at a 95% confidence level.
3. Once normality was verified, a normal distribution was fitted to each data sample. The mean (μ) of this distribution was the value of the safety factor for each case.
4. Finally, the quality of the adjustment was verified with the Kolmogorov–Smirnov test, a *p*-value higher than 0.05 indicating an adequate adjustment quality at a confidence level of 95%.

Table 14 shows the results of the safety-factor evaluation. Data always followed a normal distribution according to all the hypothesis tests, as required for an adequate calculation of safety factors [57]. Focusing on the safety factors, the value for the mean expected values was always approximately 1, indicating that overall the fit was accurate [44]. For the minimum expected values, the value reached depended on the quality of the fit. Thus, the model for the modulus of elasticity presented a safety factor of around 1.13, while the safety factors for tensile splitting and compressive strengths were 1.19 and 1.23, respectively. Thus, it can be stated that non-linear multiple regression allowed the development of adequate models to estimate these three mechanical properties by NDT, as the models provided greater safety margins for such properties for which the regression adjustment did not yield such high accuracy [51, 53].

5.5.3 Model validation through a robustness analysis

The first validation of the optimal models developed through non-linear multiple regression was a robustness analysis. For this purpose, a percentage variation in the values of the NDT properties, 1% for UPV and 3% for rebound index, both positive and negative, was assumed. Then, the estimated values of the mechanical properties were calculated with the resulting values of the NDT properties, and subsequently compared with the experimental results. The percentage variation of each NDT property was defined by first calculating the overall mean value as the average of the values of that NDT property for all the concrete mixtures; secondly calculating the overall standard deviation as the average of the standard deviations of all the mixes for that NDT property; and finally determining the percentage of the overall mean value of the NDT property that represented the overall standard deviation [40].Figure 13 shows the comparison between the experimental and estimated values from this robustness analysis for compressive strength, for which both individual and combined variations of the NDT properties were considered. Figure 14 depicts such comparison for modulus of elasticity and tensile splitting strength, in which only UPV variation were considered. Table 15 shows the deviations and safety factors for the expected mean values resulting from this robustness analysis.

The deviations from the robustness analysis were generally adequate [40], with values around 5–6% in most cases. Furthermore, the percentage of experimental results estimated with an accuracy of ± 10% was adequate, generally higher than 75.0%, and the minimum expected value was always lower than the experimental one (safety prediction of 100%). The only property that did not follow these trends in some cases was compressive strength, which showed a mean deviation of 7.1% when a simultaneous positive variation of both NDT properties was assumed, and a mean deviation of 6.9% when both NDT properties experienced a simultaneous negative variation. The dependence of the model for compressive strength on both UPV and rebound index caused the prediction accuracy to decrease more markedly when both NDT properties simultaneously experienced a variation of the same sign [40]. In terms of safety factors, the positive variation of the NDT properties led to safety factors below 1, although they were mostly close enough to 1 to ensure a proper estimation safety [57]. The most unfavorable situation was a positive variation of the rebound index when estimating compressive strength, regardless of the UPV variation, due to the fact that this NDT property shows greater experimental variability

 https://doi.org/10.1007/s43452-026-01442-4

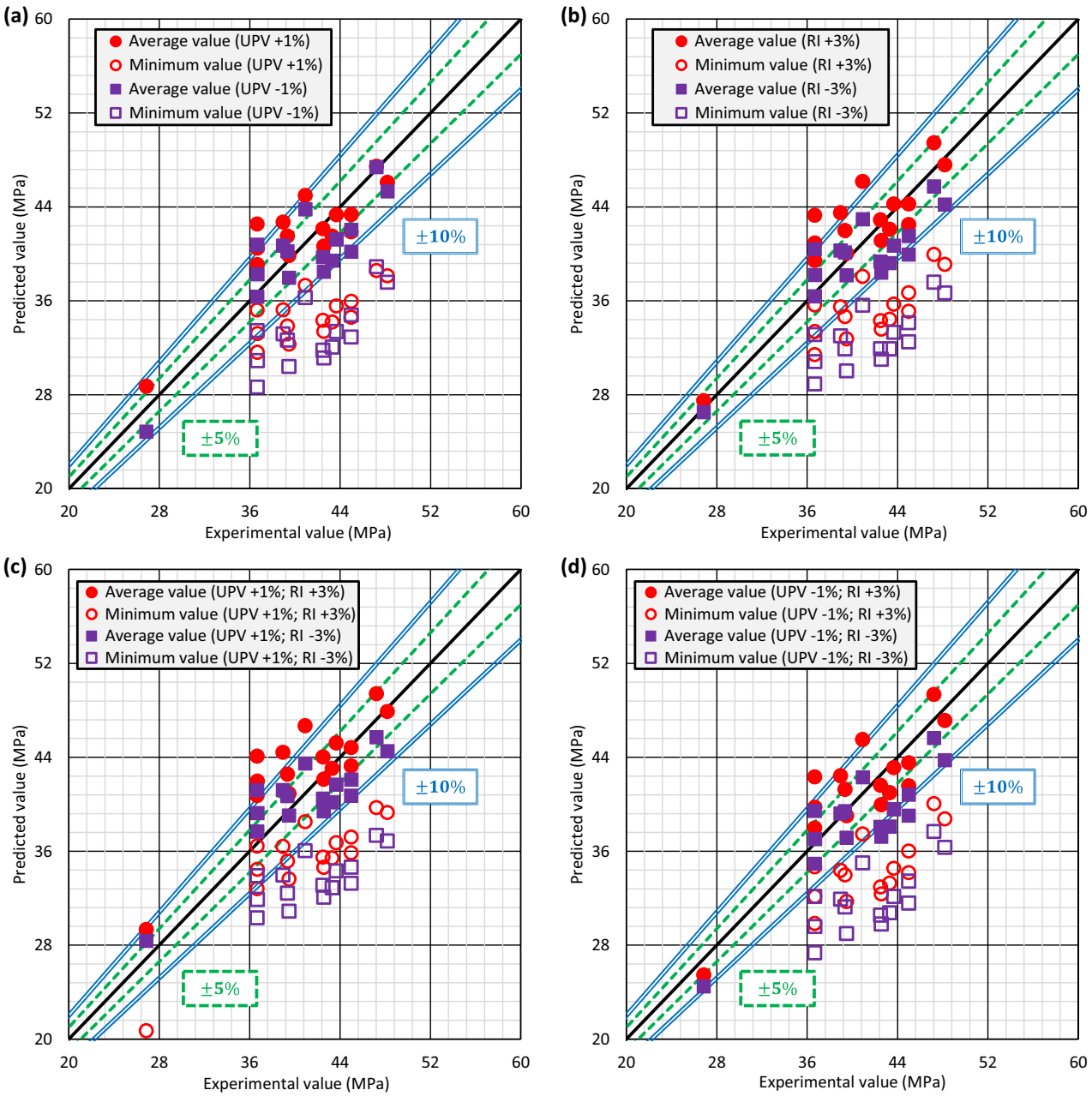

Fig. 13 Robustness evaluation of non-linear multiple-regression models dependent on UPV and rebound index (compressive-strength model): (a) UPV variations; (b) rebound-index variations; (c) and (d) simultaneous UPV and rebound-index variations. Legend: *UPV* ultrasonic pulse velocity, *RI* rebound index

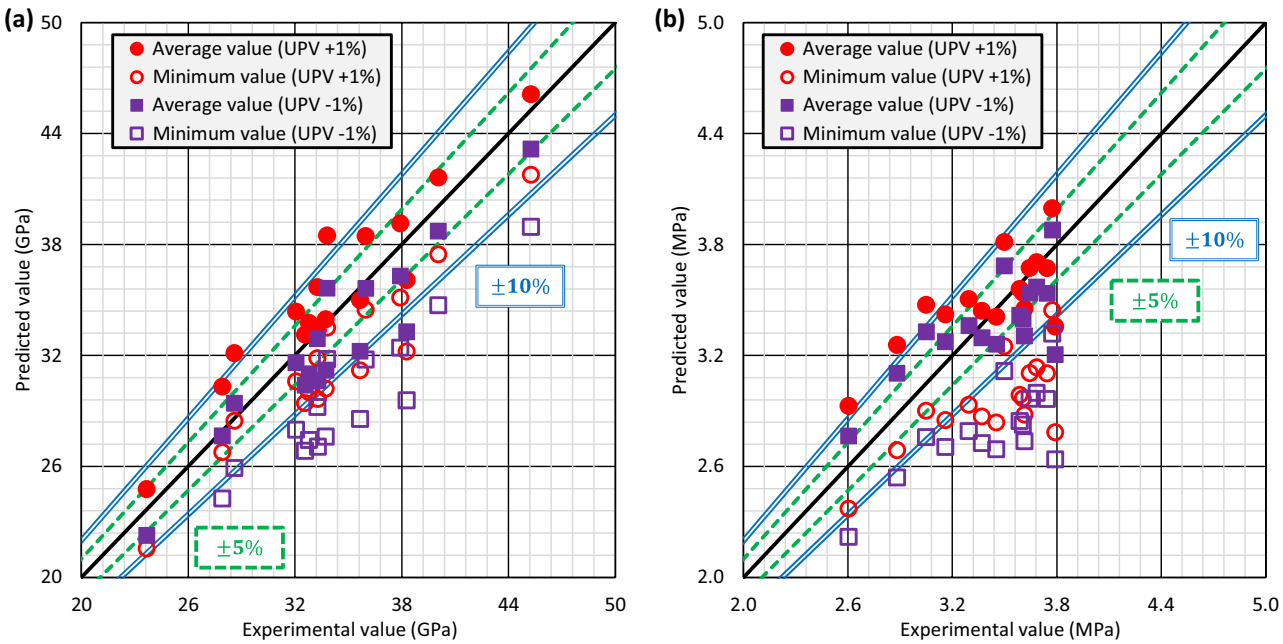

Fig. 14 Robustness evaluation of non-linear multiple-regression models dependent exclusively on UPV: (a) modulus of elasticity; (b) tensile splitting strength. Legend: *UPV* ultrasonic pulse velocity

Table 15 Robustness evaluation of non-linear multiple-regression models through deviations and safety factors

Mechanical property	Hypothesis	Mean deviation (%)	5%-accuracy predictions (%)	10%-accuracy predictions (%)	Safety prediction (%)	χ^2 *p*-value for safety factor	Safety factor for mean expected value
Compressive strength	UPV+1%	5.7	50.0	87.5	100	0.5341	0.9781
	UPV -1%	6.0	37.5	87.5	100	0.1866	1.0268
	RI+3%	5.9	56.3	75.0	100	0.3925	0.9646
	RI -3%	5.8	43.8	87.5	100	0.5341	1.0321
	UPV+1% and RI+3%	7.1	56.3	68.8	100	0.3925	0.9442
	UPV+1% and RI -3%	5.9	37.5	93.8	100	0.6890	1.0089
	UPV -1% and RI+3%	5.7	50.0	87.5	100	0.2757	0.9896
	UPV -1% and RI -3%	6.9	37.5	75.0	100	0.1223	1.0605
Modulus of elasticity	UPV+1%	5.2	56.3	87.5	100	0.6890	0.9709
	UPV -1%	5.0	50.0	93.8	100	0.8343	1.0437
Tensile splitting strength	UPV+1%	5.9	50.0	75.0	100	0.8343	0.9732
	UPV -1%	5.7	43.8	93.8	100	0.2757	1.0147

than UPV [32, 54]. In view of these aspects, it is advisable when estimating the mechanical behavior of concrete simultaneously containing CRA and RCWTB to directly use the measured value of UPV, since small variations of this NDT property did not affect estimation quality, and to slightly reduce the recorded value of rebound index to minimize the probability of overestimating compressive strength.

5.5.4 Model validation through random association

The second validation to which the non-linear multiple-regression models were subjected was random association. For this purpose, the values of the properties measured in each individual specimen were considered. Then, each individual value for every mechanical property of each concrete mix was randomly associated with an

 https://doi.org/10.1007/s43452-026-01442-4

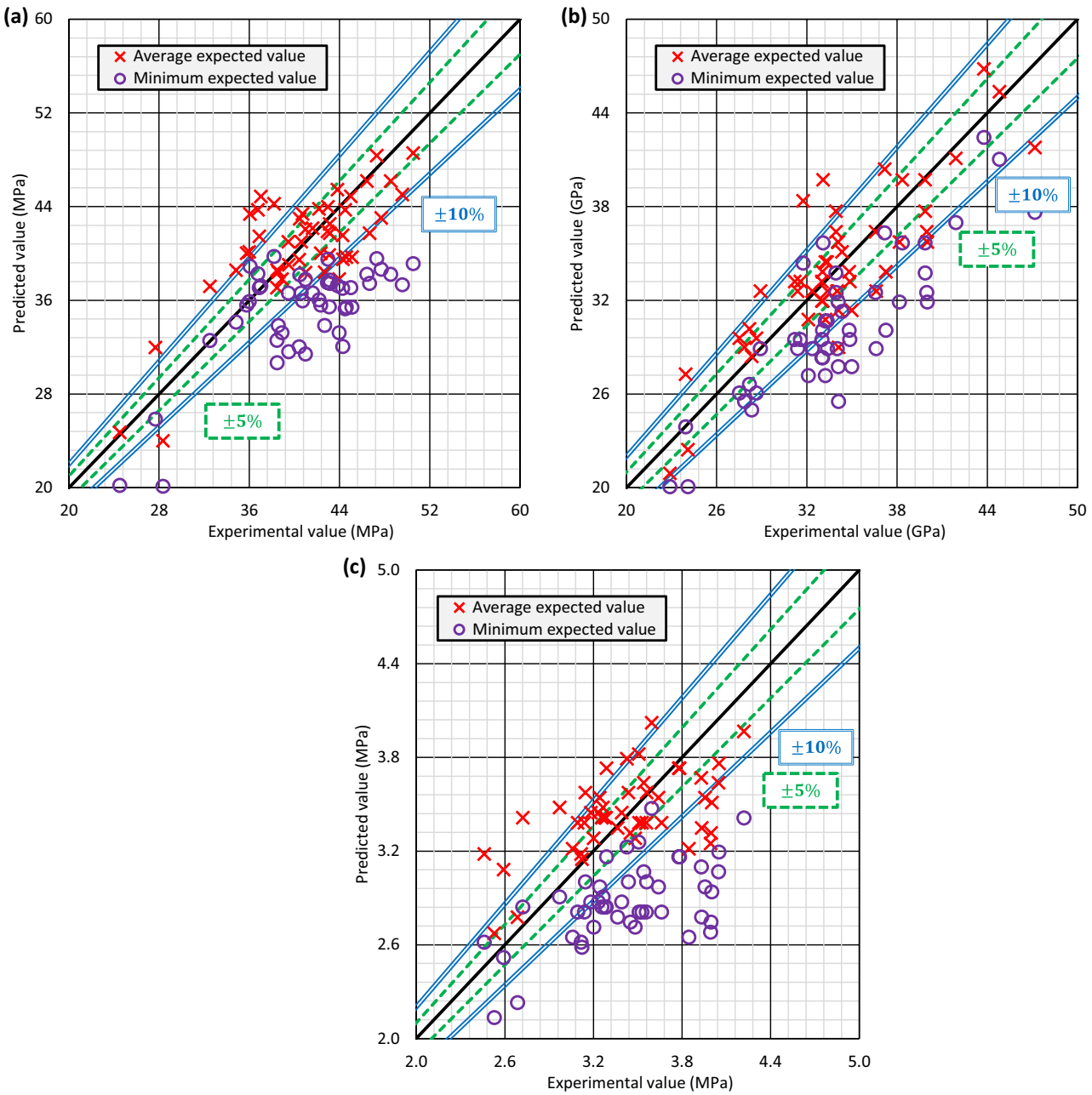

Fig. 15 Evaluation through random association of non-linear multiple-regression models: (a) compressive strength; (b) modulus of elasticity; (c) tensile splitting strength

Table 16 Random-association evaluation of non-linear multiple-regression models through deviations and safety factors

Mechanical property	Mean deviation (%)	5%-accuracy predictions (%)	10%-accuracy predictions (%)	Safety prediction (%)	χ^2 p-value for safety factor	Safety factor for mean expected value
Compressive strength	7.2	47.9	64.6	87.5	0.7872	1.0019
Modulus of elasticity	6.4	47.9	79.2	95.8	0.5637	1.0032
Tensile splitting strength	8.2	39.6	68.8	95.8	0.9642	0.9932

individual value of UPV and rebound index of that same mix. The mechanical properties were estimated through these pairs of values of the NDT properties, and compared with the experimental values with which they were associated. Figure 15 shows the comparison between the experimental and estimated values, while Table 16 details the deviations and safety factors for the mean expected values.

As expected, the estimation accuracy decreased compared to that yielded in the development of the models (Table 13). Nevertheless, the models performed adequately, exhibiting mean deviations with a maximum value of around 8%, below the usual limit of 10% [38]. In addition, 65–80% of the experimental results were predicted with an accuracy of ± 10%, the minimum expected value was lower than the experimental value in around 90% of the cases, and the safety factors for the mean expected values were around 1. These values were adequate to the limits established in the literature when performing this type of validation [40, 55, 57], thus emphasizing the adequacy of the models developed through non-linear multiple regression for the NDT estimation of the mechanical properties of concrete simultaneously containing CRA and RCWTB.

6 Conclusions

This research has evaluated the validity of Ultrasonic Pulse Velocity (UPV) and rebound index to assess the mechanical behavior (compressive strength, modulus of elasticity, Poisson's coefficient, tensile splitting strength, and flexural strength) of concrete made with up to 100% Coarse Recycled Aggregate (CRA) and 10% Raw-Crushed Wind-Turbine Blade (RCWTB). For this purpose, an experimental plan was conducted to measure all these properties, results that were subsequently used to analyze the relationship between mechanical and Non-Destructive Testing (NDT) properties through Response Surface Methodology (RSM) and regression approaches. The following conclusions can be drawn:

- UPV consistently decreased with increasing CRA and RCWTB contents in concrete due to the reduction in density and increase in porosity caused by both wastes. However, rebound index did not show such a clear trend, presenting a greater experimental variability, as these wastes did not notably impact the hardness of the cementitious matrix, the surface hardness of concrete being only affected by punctual particles of both wastes.
- The RSM models for predicting UPV from the contents of CRA and RCWTB were adequate, reaching R^2 coefficients higher than 90%. However, the RSM models for rebound index were not significant, with R^2 coefficients of only around 50%. This discrepancy arose because UPV showed clear variation trends when both wastes were added, while rebound index exhibited large experimental variability. An α value of ± 1 was the most appropriate for the central composite design used for RSM development.
- RSM models showed an almost complete coincidence between the directions of maximum variation (gradients) of UPV and modulus of elasticity, which also coincided with those of compressive strength and tensile splitting strength when high waste amounts were incorporated. The rebound-index gradient coincided with that of compressive strength when low RCWTB contents were added. Thus, RSM demonstrated that UPV was precisely related to these three mechanical properties, while rebound index only showed a connection with compressive strength.
- Analyses through simple regression and linear multiple regression revealed that significant models to predict Poisson's coefficient and flexural strength could not be developed. UPV and rebound index did not properly approach the stitching effect of the fibers from glass fiber-reinforced polymer contained in RCWTB, which impacted these mechanical properties. Compressive strength, modulus of elasticity and tensile splitting strength could be successfully estimated by UPV, as these mechanical properties depended mainly on phenomena related to the cementitious matrix. The incorporation of rebound index to the models only improved the estimation accuracy for compressive strength. Modulus of elasticity was always estimated with the highest accuracy.
- Non-linear multiple regression demonstrated the feasibility of accurately estimating compressive strength, modulus of elasticity and tensile splitting strength of concrete made simultaneously with CRA and RCWTB

through NDT. These models showed a linear nature in the study space, a feature also verified by correlations. In addition, the safety factors for the minimum estimated values were always adequate, providing a greater safety margin for the less accurate models.

Overall, it can be concluded that Poisson's coefficient and flexural strength of concrete simultaneously containing CRA and RCWTB could not be estimated by UPV and rebound index. However, the estimation of compressive strength, modulus of elasticity and tensile splitting strength was accurate and safe, UPV being the NDT property that was most effectively linked to these mechanical properties. The rebound index improved the estimation accuracy of compressive strength, but it is advisable to reduce the experimentally measured value of this NDT property to avoid overestimations.

Acknowledgements This research work was supported by grant TED2021-129715B-I00 funded by MICIU/AEI/https://doi.org/10.13039/501100011033 and by European Union NextGenerationEU/PRTR; grant PID2023-146642OB-I00 funded by MICIU/AEI/https://doi.org/10.13039/501100011033 and by ERDF/EU; grants UIC-231 and BU033P23 funded by the Junta de Castilla y León (Regional Government) and ERDF/EU; and grant SUCONS, Y135.GI funded by the University of Burgos.

Funding Open access funding provided by FEDER European Funds and the Junta de Castilla y León under the Research and Innovation Strategy for Smart Specialization (RIS3) of Castilla y León 2021-2027.

Data availability The authors declare that the data supporting the findings of this study are available within the paper. The authors are available for further clarifications.

Declarations

Conflict of interest The authors declare that they have no known competing financial interests or personal relationships that could have appeared to influence the work reported in this paper.

References

1. Patil YR, Dakwale VA, Ralegaonkar RV. Recycling construction and demolition waste in the sector of construction. Adv Civil Eng. 2024;2024:6234010. https://doi.org/10.1155/2024/6234010.
2. Agrela F, Sánchez De Juan M, Ayuso J, Geraldes VL, Jiménez JR. Limiting properties in the characterisation of mixed recycled aggregates for use in the manufacture of concrete. Constr Build Mater. 2011;25(10):3950–5. https://doi.org/10.1016/j.conbuildmat.2011.04.027.
3. Faleschini F, Jiménez C, Barra M, Aponte D, Vázquez E, Pellegrino C. Rheology of fresh concretes with recycled aggregates. Constr Build Mater. 2014;73:407–16. https://doi.org/10.1016/j.conbuildmat.2014.09.068.
4. Xu G, Zhang Z, Li J, Tian Q, Cai J, Guo S, et al. Design and preparation methods for high-performance recycled aggregate concrete: a review. Proc Inst Civ Eng Waste Resour Manag. 2024;178(1):1–19. https://doi.org/10.1680/jwarm.23.00034.
5. Kumari P, Paruthi S, Alyaseen A, Husain Khan A, Jijja A. Predictive performance assessment of recycled coarse aggregate concrete using artificial intelligence: a review. Clean Mater. 2024;13:100263. https://doi.org/10.1016/j.clema.2024.100263.
6. Zheng Y, Zhang Y, Zhang P. Methods for improving the durability of recycled aggregate concrete: a review. J Mater Res Technol. 2021;15:6367–86. https://doi.org/10.1016/j.jmrt.2021.11.085.

7. Silva RV, De Brito J, Dhir RK. Prediction of the shrinkage behavior of recycled aggregate concrete: a review. Constr Build Mater. 2015;77:327–39. https://doi.org/10.1016/j.conbuildmat.2014.12.102.
8. Salesa Á, Pérez-Benedicto JA, Colorado-Aranguren D, López-Julián PL, Esteban LM, Sanz-Baldúz LJ, et al. Physico—mechanical properties of multi—recycled concrete from precast concrete industry. J Clean Prod. 2017;141:248–55. https://doi.org/10.1016/j.jclepro.2016.09.058.
9. Fiol F, Thomas C, Muñoz C, Ortega-López V, Manso JM. The influence of recycled aggregates from precast elements on the mechanical properties of structural self-compacting concrete. Constr Build Mater. 2018;182:309–23. https://doi.org/10.1016/j.conbuildmat.2018.06.132.
10. Liu Z, Zhao YG, Ma L, Lin S. Review on high-strength recycled aggregate concrete: mix design, properties, models and structural behaviour. Structures. 2024;64:106598. https://doi.org/10.1016/j.istruc.2024.106598.
11. Aghaee K, Khayat KH. Effect of shrinkage-mitigating materials on performance of fiber-reinforced concrete—an overview. Constr Build Mater. 2021;305:124586. https://doi.org/10.1016/j.conbuildmat.2021.124586.
12. Sonar K, Sathe S. Exploring fiber reinforcements in concrete and its challenges: a comprehensive review. Multiscale Multidiscip Model Exp Design. 2024;7(4):3099–131. https://doi.org/10.1007/s41939-024-00404-8.
13. Zheng Y, Lv X, Hu S, Zhuo J, Wan C, Liu J. Mechanical properties and durability of steel fiber reinforced concrete: a review. J Build Eng. 2024;82:108025. https://doi.org/10.1016/j.jobe.2023.108025.
14. Manso-Morato J, Hurtado-Alonso N, Revilla-Cuesta V, Skaf M, Ortega-López V. Fiber-reinforced concrete and its life cycle assessment: a systematic review. J Build Eng. 2024;94:110062. https://doi.org/10.1016/j.jobe.2024.110062.
15. Shen Y, Apraku SE, Zhu Y. Recycling and recovery of fiber-reinforced polymer composites for end-of-life wind turbine blade management. Green Chem. 2023;25(23):9644–58. https://doi.org/10.1039/d3gc03479h.
16. Rani M, Choudhary P, Krishnan V, Zafar S. A review on recycling and reuse methods for carbon fiber/glass fiber composites waste from wind turbine blades. Compos Part B Eng. 2021;215:108768. https://doi.org/10.1016/j.compositesb.2021.108768.
17. Joustra J, Flipsen B, Balkenende R. Structural reuse of wind turbine blades through segmentation. Compos Part C Open Access. 2021;5:100137. https://doi.org/10.1016/j.jcomc.2021.100137.
18. Fonte R, Xydis G. Wind turbine blade recycling: an evaluation of the European market potential for recycled composite materials. J Environ Manage. 2021;287:112269. https://doi.org/10.1016/j.jenvman.2021.112269.
19. Wei Y, Hadigheh SA. Enhancing carbon fibre recovery through optimised thermal recycling: kinetic analysis and operational parameter investigation. Mater Today Sustain. 2024;25:100661. https://doi.org/10.1016/j.mtsust.2023.100661.
20. Tao Y, Hadigheh SA, Wei Y. Recycling of glass fibre reinforced polymer (GFRP) composite wastes in concrete: a critical review and cost benefit analysis. Structures. 2023;53:1540–56. https://doi.org/10.1016/j.istruc.2023.05.018.
21. Yu T, Zhou C, Cao L, Zhang Y, Cao P, Shi F. Effect of GFRP fibres recovered from decommissioned wind turbine blades on the fracture properties of concrete. Constr Build Mater. 2025;463:140121. https://doi.org/10.1016/j.conbuildmat.2025.140121.
22. Zhang F, Lu Z, Wang D. Working and mechanical properties of waste glass fiber reinforced self-compacting recycled concrete. Constr Build Mater. 2024;439:137172. https://doi.org/10.1016/j.conbuildmat.2024.137172.
23. Liu P, Barlow CY. Wind turbine blade waste in 2050. Waste Manag. 2017;62:229–40. https://doi.org/10.1016/j.wasman.2017.02.007.
24. Trento D, Faleschini F, Revilla-Cuesta V, Ortega-López V. Improving the early-age behavior of concrete containing coarse recycled aggregate with raw-crushed wind-turbine blade. J Build Eng. 2024;92:109815. https://doi.org/10.1016/j.jobe.2024.109815.
25. Kaboglu C, Pimenta S, Morris A, Dear JP. The effect of different types of core material on the flexural behavior of sandwich composites for wind turbine blades. J Therm Eng. 2017;3(2):1102–9. https://doi.org/10.18186/thermal.298608.
26. Xu MX, Ji HW, Meng XX, Yang J, Wu YC, Di JY, et al. Effects of core materials on the evolution of products during the pyrolysis of end-of-life wind turbine blades. J Anal Appl Pyrolysis. 2023;175:106222. https://doi.org/10.1016/j.jaap.2023.106222.
27. Baturkin D, Hisseine OA, Masmoudi R, Tagnit-Hamou A, Massicotte L. Valorization of recycled FRP materials from wind turbine blades in concrete. Resour Conserv Recycl. 2021;174:105807. https://doi.org/10.1016/j.resconrec.2021.105807.
28. Revilla-Cuesta V, Skaf M, Ortega-López V, Manso JM. Raw-crushed wind-turbine blade: waste characterization and suitability for use in concrete production. Resour Conserv Recycling. 2023;198:107160. https://doi.org/10.1016/j.resconrec.2023.107160.
29. Hurtado-Alonso N, Manso-Morato J, Revilla-Cuesta V, Skaf M. Strength-based RSM optimization of concrete containing coarse recycled concrete aggregate and raw-crushed wind-turbine blade. Compos Struct. 2025;356:118895. https://doi.org/10.1016/j.compstruct.2025.118895.
30. Ortega-López V, Faleschini F, Manso JM, Revilla-Cuesta V. Bending performance of concrete with coarse recycled aggregate and raw-crushed wind-turbine blade at an early age. Arch Civ Mech Eng. 2025;25(4):165. https://doi.org/10.1007/s43452-025-01215-5.

31. Schmid S, Hachmann C, Boehm C, Krischer L, Mendler A, Kollofrath J, et al. Estimating Young's moduli based on ultrasound and full-waveform inversion. Ultrasonics. 2024;136:107165. https://doi.org/10.1016/j.ultras.2023.107165.
32. Kolek J. An appreciation of the Schmidt rebound hammer. Mag Concr Res. 1958;10(28):27–36. https://doi.org/10.1680/macr.1958.10.28.27.
33. Sokołowska JJ, Załęgowski K, Czarnecki L. Measuring of the polymer concrete maturity using non-destructive ultrasonic method. Arch Civ Mech Eng. 2025;25(4):240. https://doi.org/10.1007/s43452-025-01285-5.
34. Rahmati M, Toufigh V, Keyvan K. Monitoring of crack healing in geopolymer concrete using a nonlinear ultrasound approach in phase-space domain. Ultrasonics. 2023;134:107095. https://doi.org/10.1016/j.ultras.2023.107095.
35. Ali-Benyahia K, Kenai S, Ghrici M, Sbartaï ZM, Elachachi SM. Analysis of the accuracy of in-situ concrete characteristic compressive strength assessment in real structures using destructive and non-destructive testing methods. Constr Build Mater. 2023;366:130161. https://doi.org/10.1016/j.conbuildmat.2022.130161.
36. Ottosen LM, Kunther W, Ingeman-Nielsen T, Karatosun S. Non-destructive testing for documenting properties of structural concrete for reuse in new buildings: a review. Materials. 2024;17(15):3814. https://doi.org/10.3390/ma17153814.
37. Kazemi M, Madandoust R, de Brito J. Compressive strength assessment of recycled aggregate concrete using Schmidt rebound hammer and core testing. Constr Build Mater. 2019;224:630–8. https://doi.org/10.1016/j.conbuildmat.2019.07.110.
38. Espinosa AB, Revilla-Cuesta V, Skaf M, Faleschini F, Ortega-López V. Utility of ultrasonic pulse velocity for estimating the overall mechanical behavior of recycled aggregate self-compacting concrete. Appl Sci. 2023;13(2):874. https://doi.org/10.3390/app13020874.
39. Singh N, Singh SP. Evaluating the performance of self compacting concretes made with recycled coarse and fine aggregates using non destructive testing techniques. Constr Build Mater. 2018;181:73–84. https://doi.org/10.1016/j.conbuildmat.2018.06.039.
40. Revilla-Cuesta V, Shi JY, Skaf M, Ortega-López V, Manso JM. Non-destructive density-corrected estimation of the elastic modulus of slag-cement self-compacting concrete containing recycled aggregate. Dev Built Environ. 2022;12:100097. https://doi.org/10.1016/j.dibe.2022.100097.
41. Bawa S, Alam P, Saini S. Evaluation of performance of hybrid fiber-reinforced self-compacting concrete using non-destructive testing techniques. Innov Infrastruct Solut. 2023;8(4):126. https://doi.org/10.1007/s41062-023-01092-y.
42. Del Savio AA, La Torre Esquivel D, Carrillo J, Chi Yep E. Determination of polypropylene fiber-reinforced concrete compressive strength and elasticity modulus via ultrasonic pulse tests. Appl Sci. 2022;12(20):10375. https://doi.org/10.3390/app122010375.
43. EN-Euronorm. Rue de stassart, 36. Belgium-1050 Brussels, European Committee for Standardization.
44. EC-2. Eurocode 2: Design of concrete structures. Part 1–1: General rules and rules for buildings. CEN (European Committee for Standardization). 2010.
45. Hurtado-Alonso N, Manso-Morato J, Revilla-Cuesta V, Skaf M, Ortega-López V. Optimization of cementitious mixes through response surface method: a systematic review. Arch Civ Mech Eng. 2025;25(1):54. https://doi.org/10.1007/s43452-024-01112-3.
46. Wang W, Shen A, Lyu Z, He Z, Nguyen KTQ. Fresh and rheological characteristics of fiber reinforced concrete——a review. Constr Build Mater. 2021;296:123734. https://doi.org/10.1016/j.conbuildmat.2021.123734.
47. Islam MJ, Shahjalal M, Haque NMA. Mechanical and durability properties of concrete with recycled polypropylene waste plastic as a partial replacement of coarse aggregate. J Build Eng. 2022;54:104597. https://doi.org/10.1016/j.jobe.2022.104597.
48. Da Silva A, Kyriakides S. Compressive response and failure of balsa wood. Int J Solids Struct. 2007;44(25–26):8685–717. https://doi.org/10.1016/j.ijsolstr.2007.07.003.
49. Abd El-Malak NA. Ultrasonic properties of composites (polymer-fibre glass). Bull Mater Sci. 1997;20(7):981–90. https://doi.org/10.1007/BF02744886.
50. Stat-Ease Inc. Design Expert version 13.0.5 2025.
51. Li Z, Lu D, Gao X. Optimization of mixture proportions by statistical experimental design using response surface method—a review. J Build Eng. 2021;36:102101. https://doi.org/10.1016/j.jobe.2020.102101.
52. Statgraphics Technologies Inc. Statgraphics 19 X64. 2025.
53. Revilla-Cuesta V, Serrano-López R, Espinosa AB, Ortega-López V, Skaf M. Analyzing the relationship between compressive strength and modulus of elasticity in concrete with ladle furnace slag. Buildings. 2023;13(12):3100. https://doi.org/10.3390/buildings13123100.
54. Jones R. The ultrasonic testing of concrete. Ultrasonics. 1963;1(2):78–82. https://doi.org/10.1016/0041-624X(63)90058-1.
55. de-Prado-Gil J, Martínez-García R, Jagadesh P, Juan-Valdés A, Gónzalez-Alonso MI, Palencia C. To determine the compressive strength of self-compacting recycled aggregate concrete using artificial neural network (ANN). Ain Shams Eng J. 2024;15(2):102548. https://doi.org/10.1016/j.asej.2023.102548.

56. Bellavia S, Gratton S, Riccietti E. A Levenberg–Marquardt method for large nonlinear least-squares problems with dynamic accuracy in functions and gradients. Numer Math. 2018;140(3):791–825. https://doi.org/10.1007/s00211-018-0977-z.
57. Faleschini F, Hofer L, Belluco S, Pellegrino C. Reliability-based design of transmission and anchorage lengths in prestressed concrete elements. Struct Concr. 2023;24(3):3573–91. https://doi.org/10.1002/suco.202200604.

Authors and Affiliations

Víctor Revilla-Cuesta[1] · Manuel Hernando-Revenga[1] · Marta Skaf[2] · Ana B. Espinosa[2]

✉ Víctor Revilla-Cuesta
vrevilla@ubu.es

[1] Department of Civil Engineering, Escuela Politécnica Superior, University of Burgos, c/ Villadiego s/n, 09001 Burgos, Spain

[2] Department of Construction, Escuela Politécnica Superior, University of Burgos, c/ Villadiego s/n, 09001 Burgos, Spain